

UNITED STATES DEPARTMENT OF THE INTERIOR  
GEOLOGICAL SURVEY

Acquisition and Processing of  
Azimuthal Vertical Seismic Profiles  
at Multi-Well Experiment Site,  
Garfield County, Colorado

By M. W. Lee<sup>1</sup> and J. J. Miller<sup>1</sup>

Open-File Report 85-427

This report is preliminary and has not been reviewed for conformity with U.S. Geological Survey editorial standards and stratigraphic nomenclature. Any use of trade and company names is for descriptive purposes only and does not constitute endorsement by the U.S. Geological Survey.

<sup>1</sup>U.S. Geological Survey, Box 25046, Denver Federal Center, Denver, Colorado 80225

## CONTENTS

	Page
Abstract.....	1
Introduction.....	1
Acknowledgments.....	2
Data acquisition.....	2
Data processing.....	5
Source location 1.....	9
Source location 2.....	9
Source location 3.....	22
Source location 4.....	31
Conclusions.....	31
References cited.....	36

## ILLUSTRATIONS

Figure 1. Location of the study area and field layout.....	3
2. Craters created by airgun source.....	6
3. Comparison of monitor and downhole recordings at MWX-3 well from SL-3.....	8
4. Processing flow sheet for near-offset VSP data.....	10
5. Raw stacked vertical-component data at MWX-3 from SL-1.....	11
6. Spectrum analysis before and after variable norm deconvolution.....	12
7. Deconvolved section of data shown in figure 5, reverse polarity.....	13
8. Merged vertical-component VSP data at MWX-3 from SL-1, reversed polarity.....	14
9. Cumulative-summed vertical component of upgoing waves at MWX-3 from SL-1.....	15
10. Cumulative-summed vertical component of upgoing waves at MWX-2 from SL-1.....	16
11. Cumulative-summed and laterally stacked, vertical-component upgoing waves at MWX-3 from SL-1.....	17
12. Processing flow sheet for far-offset VSP data.....	18
13. Oriented, three-component data at MWX-3 from SL-2, reverse polarity.....	19
14. Expanded version of the vertical component data shown in figure 13, reverse polarity.....	20
15. Merged, vertical-component data at MWX-3 from SL-2.....	21
16. Schematic diagram of P-wave ray path and coordinate transformation.....	23
17. $V_1$ -component data at MWX-3 from SL-2.....	24
18. Cumulative-summed and laterally stacked, vertical component upgoing waves at MWX-3 from SL-2.....	25
19. Cumulative-summed and laterally stacked Y-component (SH-wave) data at MWX-3 from SL-2.....	26
20. Stacked, vertical-component data at MWX-3 from SL-3, reverse polarity.....	27

21. Merged, vertical-component data at MWX-3 from SL-3.....	28
22. Merged, Y-component data at MWX-3 from SL-3.....	29
23. Cumulative-summed and laterally stacked, vertical-component upgoing waves at MWX-3 from SL-3.....	30
24. Oriented, three-component data at MWX-3 from SL-4, reverse polarity.....	32
25. Merged, vertical-component data at MWX-3 from SL-4, reverse polarity.....	33
26. Cumulative-summed and laterally stacked, vertical-component upgoing waves at MWX-3 from SL-4.....	34
27. Same as figure 26 with application of spectral whitening.....	35

## TABLES

Table 1. Recording channels versus seismic component for downhole signals.....	4
2. Recording-channel assignments of surface, uphole, and monitor geophones for SL-1 and SL-3.....	4
3. Recording-channel assignments of surface, uphole, and monitor geophones for SL-2 and SL-4.....	4

# Acquisition and Processing of Azimuthal Vertical Seismic Profiles at Multi-Well Experiment Site, Garfield County, Colorado

By M. W. Lee and J. J. Miller

## ABSTRACT

An azimuthal vertical seismic profile (VSP) experiment was conducted at the Department of Energy Multi-Well Experiment (MWX) site to delineate the lenticular-type sand bodies in the Mesaverde Group. Two wells were profiled

with a tri-axial (three-component) downhole geophone and a 450 in.<sup>3</sup> surface airgun source at four different locations. In addition to VSP data, surface profile data were also collected simultaneously.

Due to poor ground conditions, malfunctioning of one of the airguns, and time limitations, the quality of the collected data is fair at best. Consequently, many difficulties were encountered in the processing and analysis of the data. This article presents the procedures used in the acquisition and processing of the azimuthal VSP data.

## INTRODUCTION

At the MWX wellsite, VSP data were collected on two separate field trips.

The first study was conducted in May 1982 at which time the data were collected from two source locations using the MWX-1 and MWX-2 wells (Lee, 1984a). The second study was conducted in April 1984 and the data were collected simultaneously at the MWX-2 and MWX-3 wells from four different source locations.

The primary objective of the 1982 trip was to collect VSP data that would be tied to three-dimensional, high-resolution surface seismic data collected previously. This data would then be used to delineate the lateral extent of the tight-gas sand bodies (Searls and others, 1983). However, analysis of the surface seismic data indicated that it is difficult to map the spatial distribution of the sand bodies primarily because of the low-frequency content of the surface data. On the other hand, the VSP data did show some possibilities for delineating the lenticular sand bodies in this area.

In April 1984, after an extensive feasibility study of mapping lenticular-type sand bodies using VSP techniques (Lee, 1984b), an azimuthal VSP survey (one near-offset VSP and three far-offset VSP's) was conducted to determine the lateral extent of the coastal sand bodies. The data acquisition section describes in detail the numerous problems encountered in the field. The second section of this report describes the processing of the azimuthal VSP data. Two VSP profiles at the MWX-2 and MWX-3 wells from the near-offset source were examined and processed. The differences between the two processed VSP profiles were not significant because the two wells were separated by only 200 ft. Some depth levels were not recorded at the MWX-2 well because of the problems with the downhole geophone. Therefore, processing of the VSP data at the MWX-3 well, and not the MWX-2 well, is presented in this report.

Data analysis and interpretation of the azimuthal VSP survey are presented in Lee (1985a).



## ACKNOWLEDGMENTS

Our sincere appreciation is extended to the CER Corporation, Sandia National Laboratory, and the Department of Energy for their support of this investigation. Particular appreciation is expressed to C. A. Searls, A. L. Sattler, J. Leinbach, N. Zihlman, D. Smith, and H. Oliver for their assistance in the data collection under adverse field conditions; also to K. Westhusing for his encouragement throughout this project.

## DATA ACQUISITION

The seismic data at MWX-2 and MWX-3 wells were digitally recorded on two MDS 10 seismic recording systems at a 1-ms sampling interval with record lengths of 5 seconds. One of these systems was owned by Geosource, Inc. and operated by their personnel under contract to the U.S. Geological Survey (USGS); the other system was USGS-owned and operated by government personnel. The seismic sources were two Bolt LSS-1T land airguns, each capable of delivering 1,500 tons of force into the ground. The seismic signal was detected in each well simultaneously by a triaxial 3-component, wall-locking geophone (one vertical and two horizontal components oriented orthogonally) designed and provided by Sandia National Laboratories.

Data from each component were amplified in two stages (high and low gain). The output of each stage modulated a constant bandwidth (4 kHz) voltage-controlled oscillator. The eight modulated signals were frequency-division multiplexed and transmitted on a single conductor wireline in each well to the surface instruments where they were demodulated. The surface instruments were interfaced with the digital seismic recorder so that each component could be recorded as a separate channel on magnetic tape in the manner of conventional reflection seismic recording. Table 1 shows the downhole signal components and their respective recording channels.

We discovered that the dynamic range of the MDS-10 system was not sufficient to record both low-gain and high-gain signals from the Sandia system. We, therefore, adjusted the dynamic range of the MDS-10 (from 48 dB to 24 dB) to optimally record the high-gain signals only.

There were four source locations distributed around the two wells as shown in figure 1. Because we had access to only two airguns, we had to shoot the wells twice. We planned to record each well from 7,000 ft to the surface at a 25-ft-depth sampling increment. The initial source configuration was one source located at source location 1 (SL-1); the other at source location 3 (SL-3). Each source was energized alternately, four times per geophone level.

Monitor geophones were placed in boreholes 100 ft below each source location in order to record the waveforms transmitted into the ground. These were to be used in the subsequent waveform-shaping processing. We also placed conventional geophone groups on the surface between the wells and each source location. The purpose of these surface spreads was to investigate the possibility of delineating sand bodies by a downward continuation method in conjunction with VSP data. Each spread consisted of groups of 6 geophones spaced 110 ft apart. Figure 1 shows the locations of the surface spreads. We needed to record two surface spreads as well as the downhole signals simultaneously; therefore, the seismic-recording system owned by the USGS was interfaced as a "slave" to the Geosource system. Table 2 lists the channels of the respective systems on which the surface spreads, uphole phones, and source monitors were recorded for SL-1 and SL-3. Table 3 lists the same information as table 2 for SL-2 and SL-4.

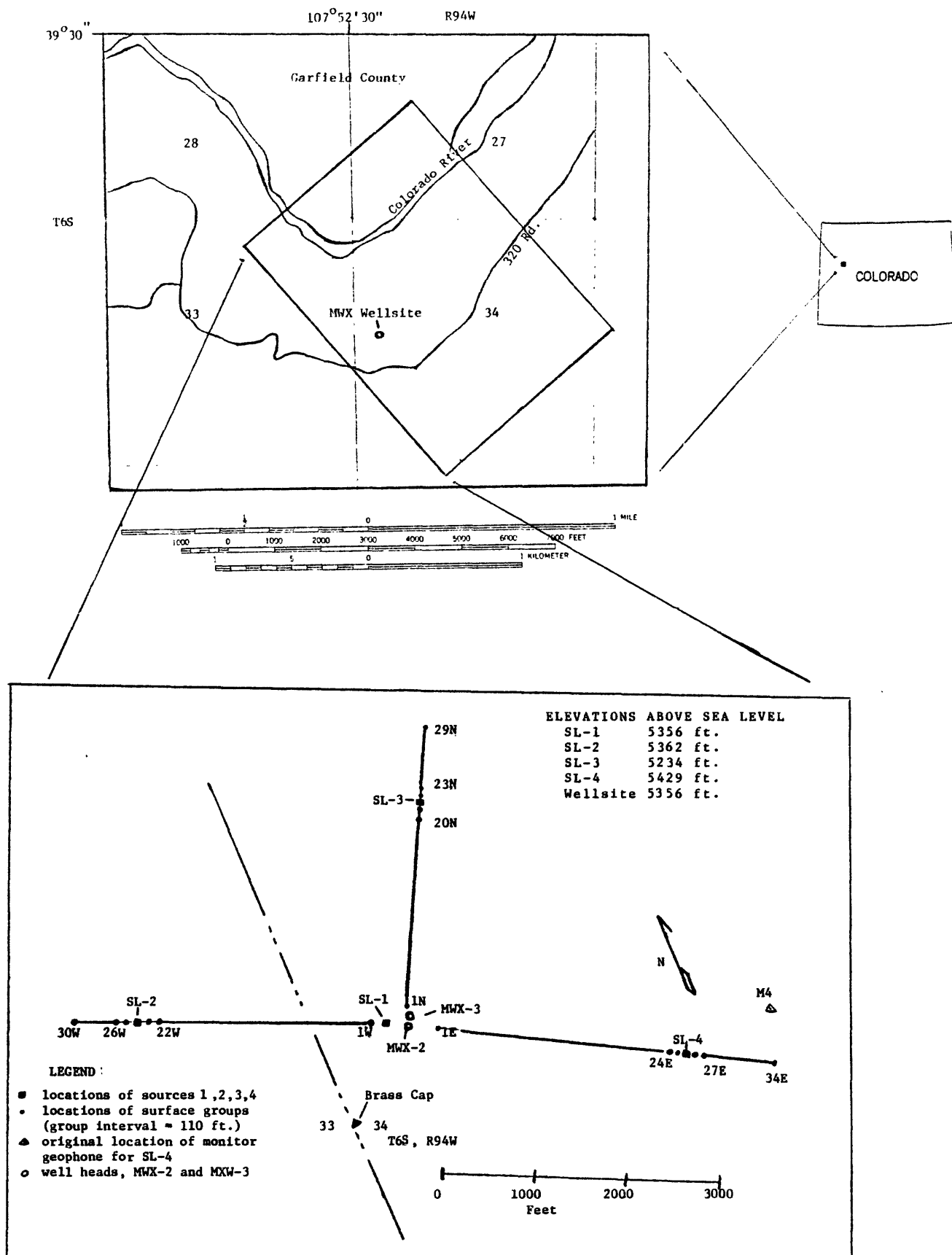


Figure 1.--Location of the study area and field layout.

Table 1.—Recording channels versus seismic component for downhole signals

GEOSOURCE RECORDING SYSTEM		
Channel number	Geophone component	Well
1	High-gain vertical	MWX-2
2	High-gain horizontal #1	MWX-2
3	High-gain horizontal #2	MWX-2
4	Low-gain vertical	MWX-2
5	Low-gain horizontal #1	MWX-2
6	Low-gain horizontal #2	MWX-2
7	High-gain vertical	MWX-3
8	High-gain horizontal #1	MWX-3
9	High-gain horizontal #2	MWX-3
10	Low-gain vertical	MWX-3
11	Low-gain horizontal #1	MWX-3
12	Low-gain horizontal #2	MWX 3

Table 2.—Recording-channel assignments of surface, uphole, and monitor geophones for source locations 1 and 3

Channel number	Record type	Recording system
13	Uphole phone for SL-1	Geosource
14	Monitor geophone, SL-1	---do---
15-17	Unused	---do---
18-37	Surface groups 1N - 20N	---do---
38	Monitor geophone, SL-3	---do---
39	Surface group 21N	---do---
40	Uphole geophone for SL-3	---do---
41-48	Surface groups 22N - 29N	---do---
1-8	Unused	USGS
9-24	Surface groups 30W - 15W	---do---
25	Unused	---do---
26	Uphole geophone SL-1	---do---
27-40	Surface groups 1W - 14W	---do---
41-48	Unused	---do---

Table 3.—Recording-channel assignments of surface, uphole, and monitor geophones for source locations 2 and 4

Channel number	Record Type	Recording system
13	Unused	Geosource
14-38	Surface groups 1E - 25E	---do---
39	Uphole geophone, SL-4	---do---
40-48	Surface groups 26E - 34E	---do---
1-6	Unused	USGS
7-12	Surface groups 30W - 25W	---do---
13	Uphole geophone, SL-2	---do---
14	Monitor geophone, SL-2	---do---
15-24	Surface groups 24W - 15W	---do---
25-26	Unused	---do---
27-40	Surface groups 1W - 14W	---do---
41-48	Unused	---do---

Processing and analysis of the surface data showed that our planned feasibility study could not be performed due to poor data quality. The irregularity of the terrain combined with high-amplitude coherent surface noise (ground roll, etc.) obliterated any usable reflections. As stated earlier, our primary goal was to record VSP data. When confronted with the many problems described next, we had little time for surface-noise analysis in the field. In any case, the surface noise was so severe that a very large geophone array would have been required to attenuate this ground noise and was not available to us.

Adverse terrain and weather conditions, in addition to equipment problems, forced us to diverge from our original plan. We had originally hoped to perform this experiment in late autumn or early winter of 1983. We chose this time period because we knew that optimum field conditions would exist (i.e., cool weather and dry ground). Circumstances beyond our control delayed the experiment until April 1984. This was the worst possible time because the ground was wet from the spring snowmelt and runoff, and the weather was unpredictable (we experienced rain, snow, sleet, and frost during the 10 days of field work). Furthermore, the local ranchers had opened up their irrigation ditches a week previously, and the fields where the airguns were located became muddy quagmires. Figure 1 shows the location of the monitor geophone for SL-4. The muddy conditions prevented the source from being located there; so we could not record a monitor geophone for this source.

The airgun trucks' weight and impact force dug deep holes in the muddy ground. The operators were forced to move the trucks as often as every 20 shots in order to avoid becoming stuck. Nevertheless, a bulldozer was needed to free the trucks on two occasions. Figure 2 shows the size, depth, and lateral extent of the holes at a typical source location. Because the trucks had to be moved as much as 200 ft from their original locations, the monitor records from source locations 2 and 3 were useless. Timing discrepancies and waveform variability due to the large number and distribution of source locations caused serious processing and interpretation problems that will be addressed in a later section. SL-1, located on the drill pad and reinforced with gravel, was the only source location that did not need to be moved extensively.

Mechanical and electronic problems also caused divergence from the original plan. The airgun at SL-3 malfunctioned due to a welding break when the downhole geophones were at the 3,000-ft level requiring two days of repairs. Therefore, the levels above 3,000 ft were shot with the airgun from SL-1 only. At the 1,000-ft level, we reduced the multiplicity to one shot per level; from 500 to 100 ft, the depth interval was changed from 25 to 50 ft in the interest of time.

During the recording of SL-2 and SL-4, a limitation on well availability forced us to reduce our multiplicity to one shot per level and a 50-ft depth interval between 2,000 and 1,000 ft depth, and to further increase the depth interval to 100 ft between 1,000 and 100 ft depths.



Figure 2.--Craters created by the airgun source

## DATA PROCESSING

Processing techniques of VSP data were discussed in detail by Lee and Balch (1983) and Lee (1984c). This section summarizes the processing of the VSP data at MWX-3 well.

The major difference between general processing procedures of VSP data and the processing procedures applied to this data was that the monitor-phone shaping filters were not included in the flow of data processing. The reason for monitor-phone shaping filter application is to remove variations of the source signatures from shot to shot. Unfortunately, no reliable monitor-phone records were derived during this field work.

Figure 3 shows the stacked downhole signal and corresponding monitor-phone signal from SL-3. Obviously, the variation observed at the monitor-phone record does not agree with the variation seen in the downhole record. This discrepancy was undoubtedly caused by the relatively large offset of the surface airgun from the monitor hole. The depth of the monitor hole was 100 ft, but the offset of the source was in the range of 100-200 ft. Because the radiation pattern of the surface airgun source is highly dependent on the vertical angle from the source to the detector, the monitor-phone did not record true downgoing longitudinal waves observed at the deep downhole geophone. Furthermore, because monitor-phone shaping filters were not applied to the data set, the amplitude variation of the processed data is partly due to the variation of the source signature and not wholly from the geological effect.

In order to resolve the variation of the source signature, we applied a variable norm deconvolution technique (Gray, 1979). Variable norm deconvolution is based on maximizing the multichannel function U, that is:

$$U(x, \alpha) = \log \prod_{j=1}^m \frac{\left[ \frac{1}{n} \sum_{i=1}^n |x_{ij}|^\alpha \right]^{n/\alpha}}{\left[ \frac{1}{n} \sum_{i=1}^n (x_{ij})^2 \right]^{n/2}},$$

where

- $\alpha$ : constant
- $m$ : number of channels,
- $n$ : number of samples, and
- $x_{ij}$ :  $i$ -th sample value at  $j$ -th channel.

When  $\alpha = 4$ , variable norm deconvolution is identical to the minimum entropy deconvolution of Wiggins (1978). The VSP data set shown here is deconvolved using  $\alpha = 3.5$ . Some of the results of this deconvolution are further discussed in the next section. The processing results are presented by source location.

The polarity convention of the VSP data display is defined as follows: Normal polarity means that the reflection from the low-impedance medium to high-impedance medium is represented as a peak; reverse polarity as a trough. Even if this polarity convention is the opposite of normal VSP recording by a wall-locking geophone, this convention is adapted here simply because it is the standard polarity convention for surface seismic profiles. Plots in the figures without any remarks are normal polarity; reverse polarity is used for clarity and is so indicated in the figures.

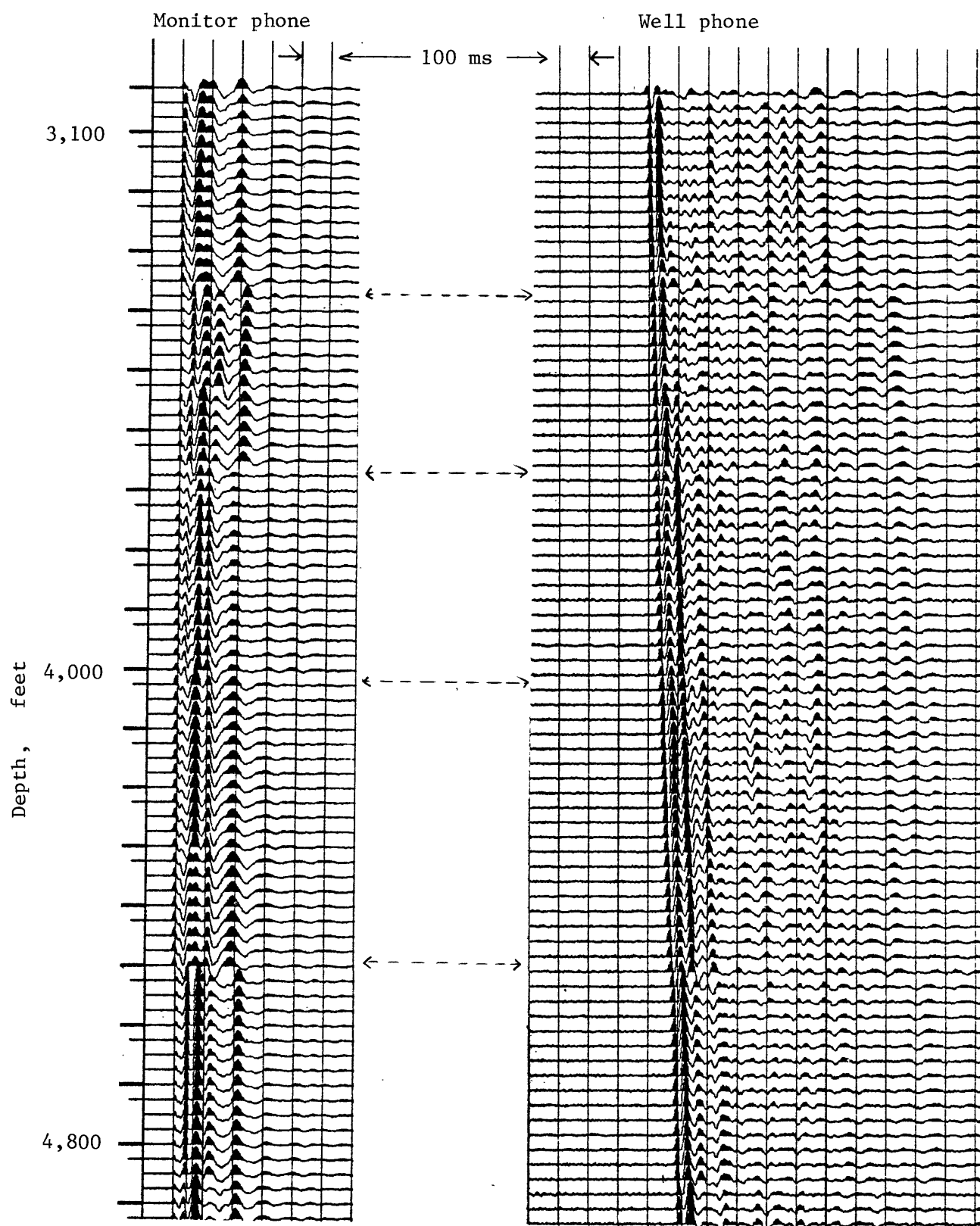


Figure 3.--Comparison of monitor and downhole recordings at MWX-3 well from SL-3.

### Source Location 1 (SL-1)

The general processing flow sheet for processing near-offset VSP data is shown in figure 4. The stacked, vertical-component data at MWX-3 well is shown in figure 5; strong, downgoing wave trains are discontinuous at several depth locations due to the variation of the near-surface condition at the source region. Based on the character changes of the downgoing wave with depth, a total of 9 deconvolution operators were derived and applied to the corresponding data set. Figure 6a shows the stacked wellphone data and its amplitude spectrum at the depth of 2,500 ft; figure 6b shows the result after various norm deconvolutions were applied. The reverberatory downgoing wave train was compressed as a simple impulse-like wavelet and the amplitude spectrum became very broad.

Figure 7 shows the deconvolved result of the data shown in figure 5. Not only did this deconvolution processing contract the long downgoing wave trains, but it also suppressed the depth-to-depth signal variations caused by source location changes.

Figure 8 shows the merged VSP section with the upgoing waves amplified by a factor of 4. The reflection from the base of the coastal zone is indicated in figures 6, 7, and 8. These three figures clearly illustrate the improvement of interpretation which can be accomplished by innovative data processing.

Cumulative-summed upgoing waves at MWX-2 and MWX-3 wells are shown in figures 9 and 10, respectively. We could not detect any significant differences between these two upgoing waves. Based on this observation and the proximity of the two well locations, we decided not to process the MWX-2 well VSP data further at this time.

Lateral stacking of VSP data (Lee, 1984c) is shown for the near-offset data in figure 11. This laterally stacked data play an important role in the interpretation of the width of the lenticular-type sand bodies in the lower coastal interval.

### Source Location 2 (SL-2)

The general processing flow sheet for far-offset VSP data is shown in figure 12. Oriented, three-component VSP data are shown in figure 13. The Z-component (vertical-component) is predominantly a longitudinal wave (P-wave); the X-component (in-line component), a vertically polarized shear wave (SV-wave); and the Y-component mainly, a horizontally polarized shear wave (SH-wave).

The expanded version of the vertical component is shown in figure 14; deconvolved, velocity-filtered, and merged VSP data with the upgoing waves amplified by a factor of 4 are shown in figure 15. Deconvolution filters performed adequately in enhancing signal-to-noise ratio for interpretation.

A static shift was applied to the data before gain application in order to suppress the arrival-time variations due to the frequent movement of the surface airgun source based on the highest and lowest apparent velocities expected in this area. This static correction was an undesirable process, but was necessary to derive a reasonable value for the interval velocity function needed in later processes, particularly for the VSP data from SL-4. This processing step was necessary due to the lack of reliable monitor records (mentioned earlier), since the monitor-shaping filters derived from these records compensate not only for the individual source waveform but also for the timing differences from the source.



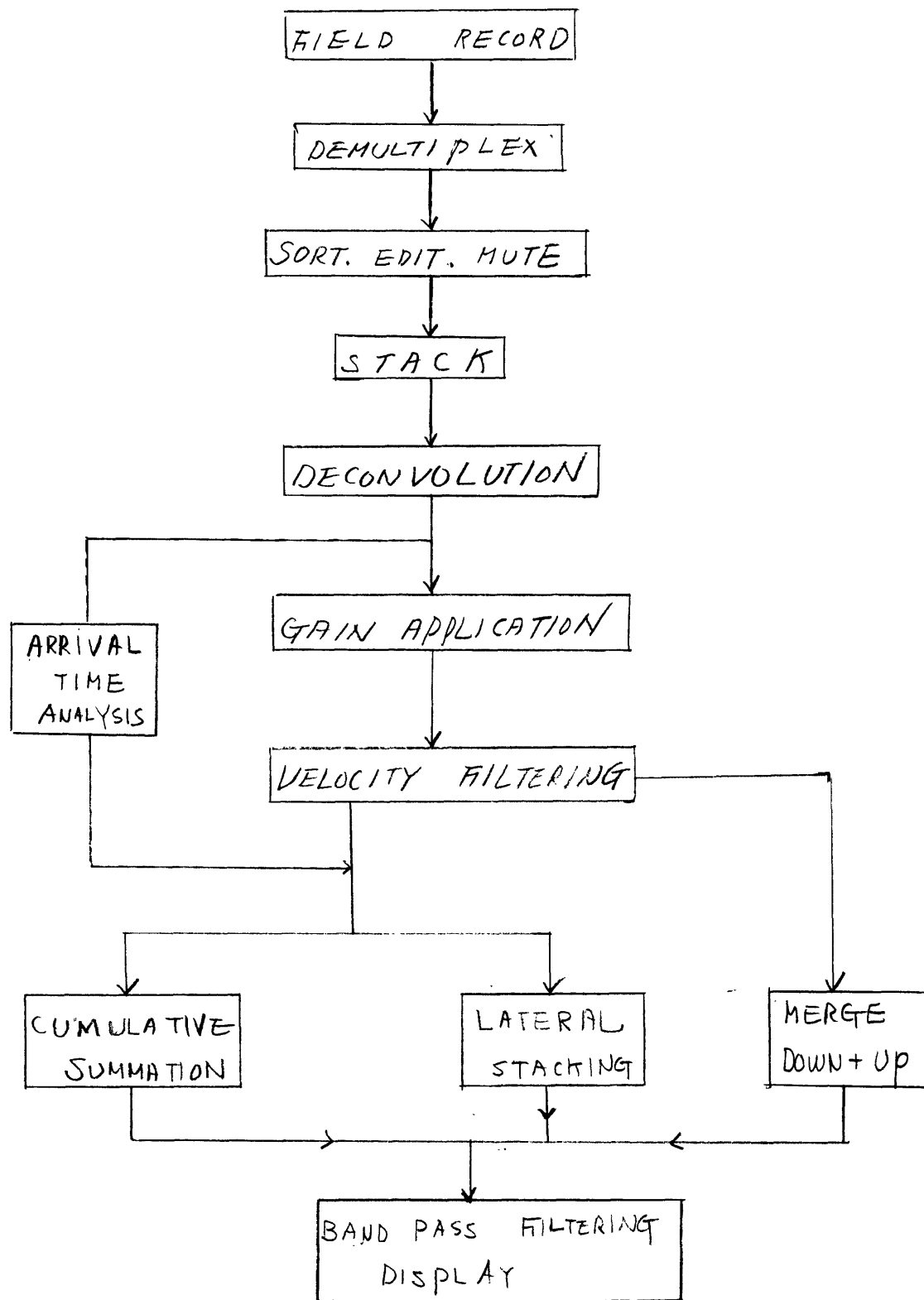


Figure 4.--Processing flow sheet for near-offset VSP data.

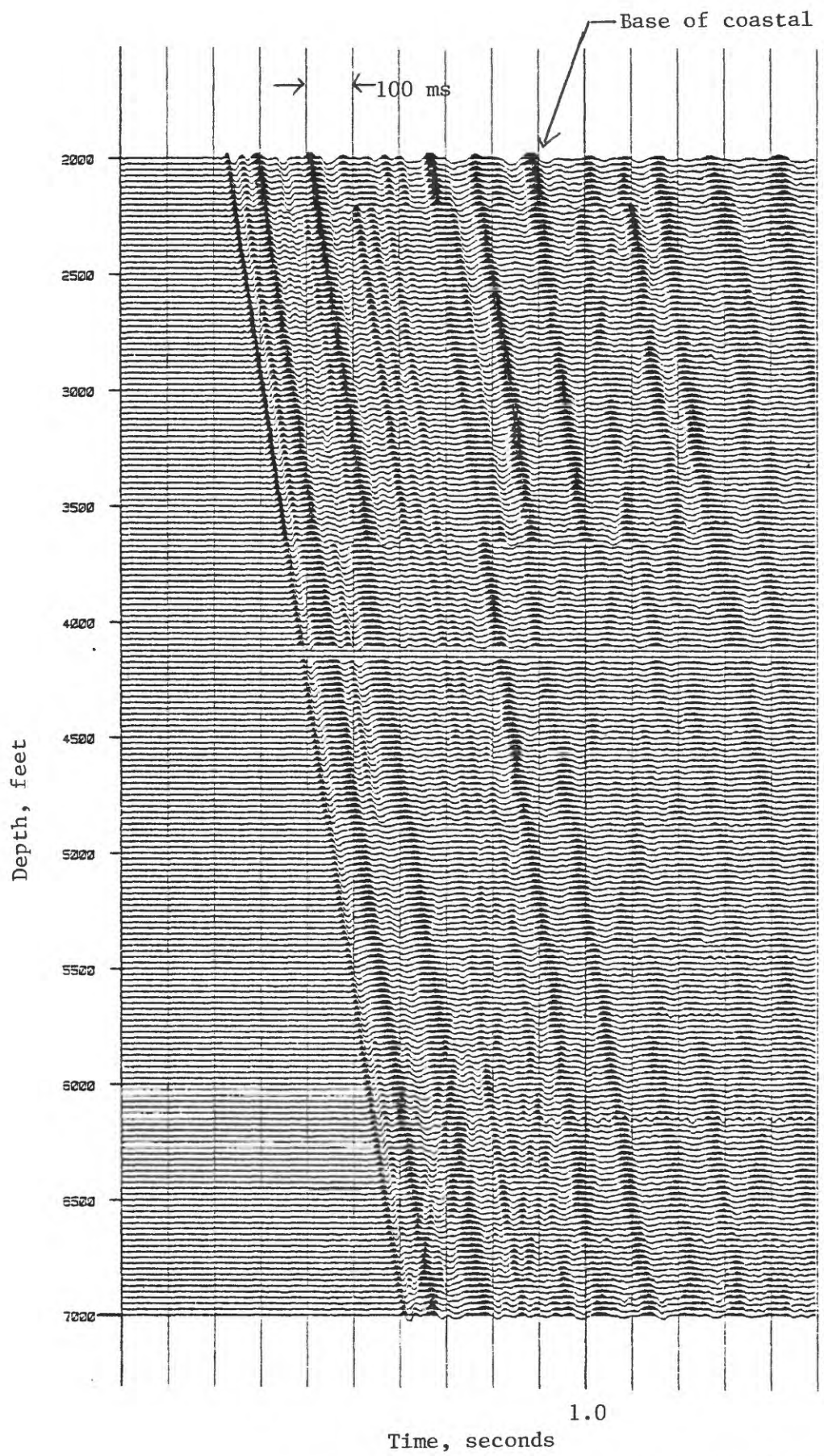


Figure 5.--Raw stacked, vertical-component data at MWX-3 from SL-1.

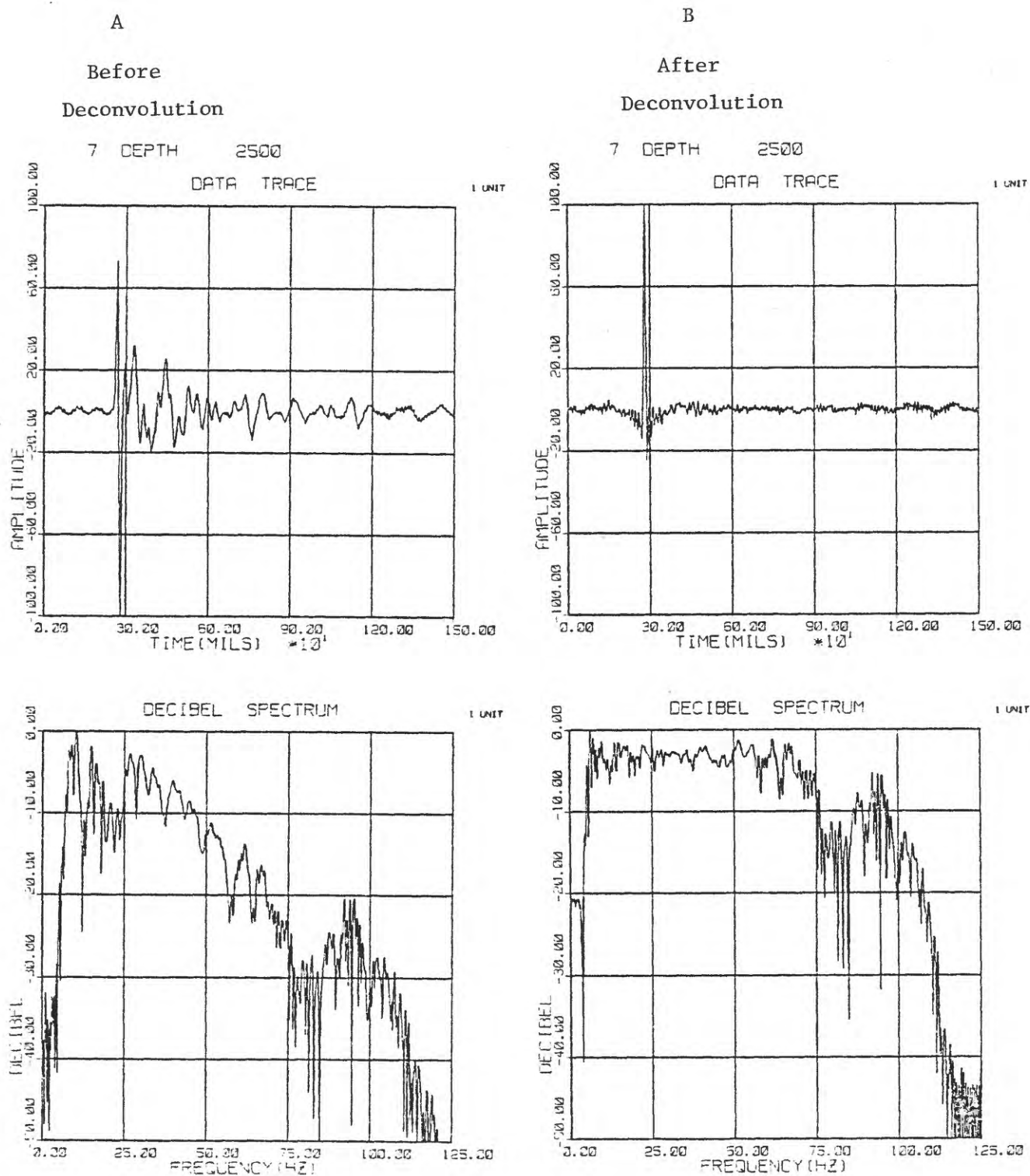


Figure 6.--Spectrum analysis before and after variable nor deconvolution at the geophone depth of 2,500 ft from SL-1.

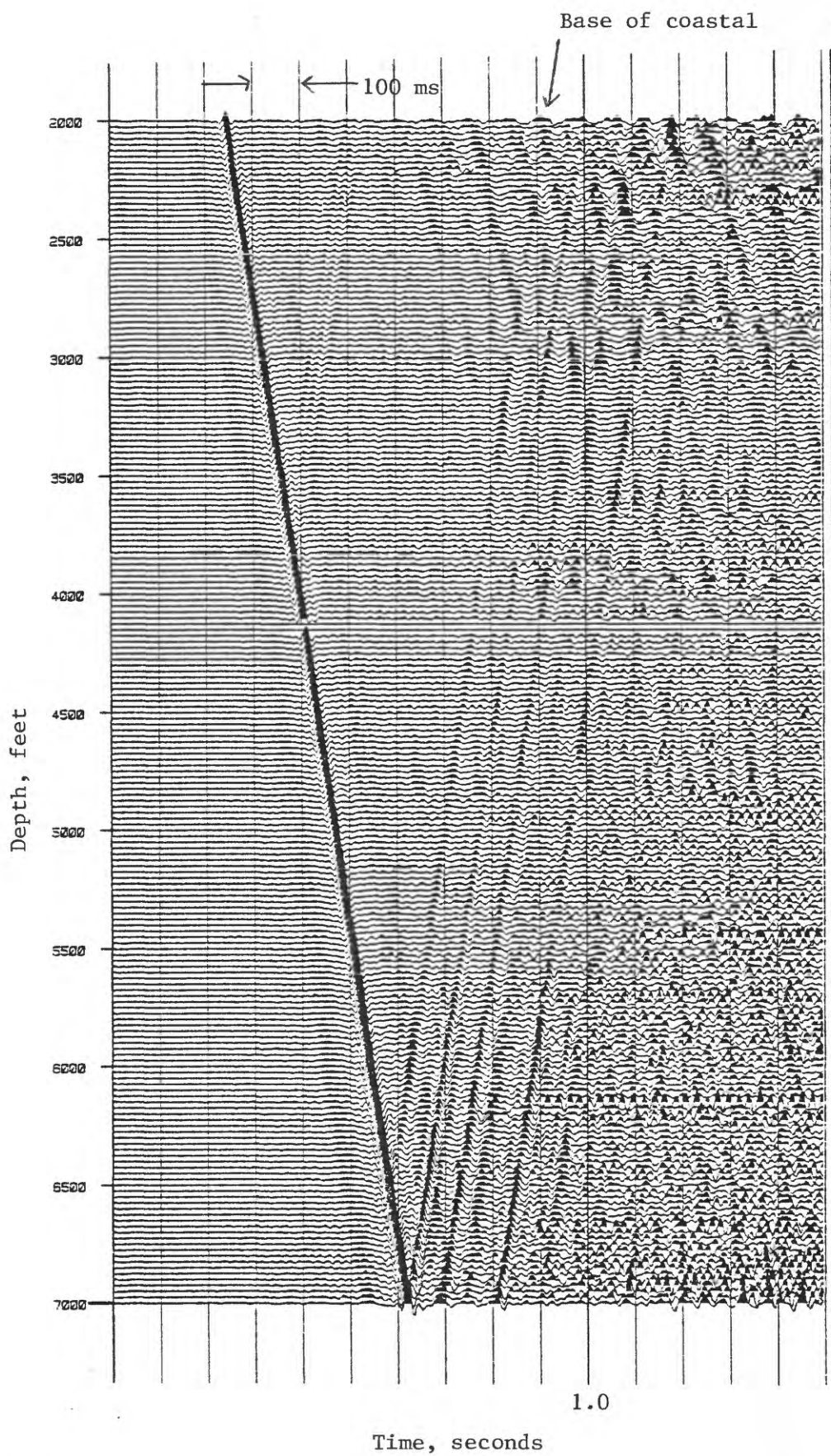


Figure 7.--Deconvolved section of data shown in figure 5, reverse polarity.



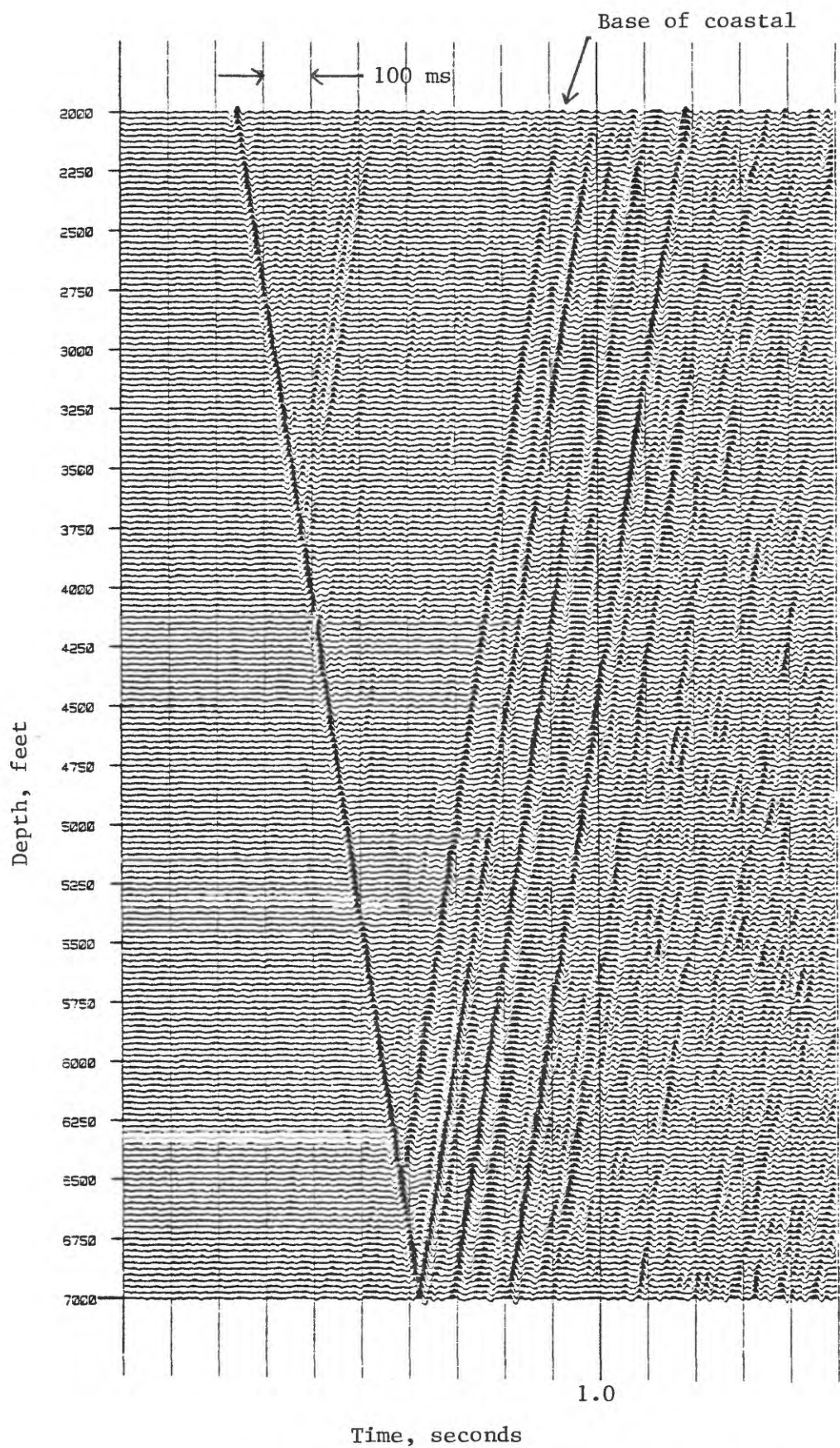


Figure 8.--Merged vertical-component VSP data at MWX-3 from SL-1, reverse polarity.

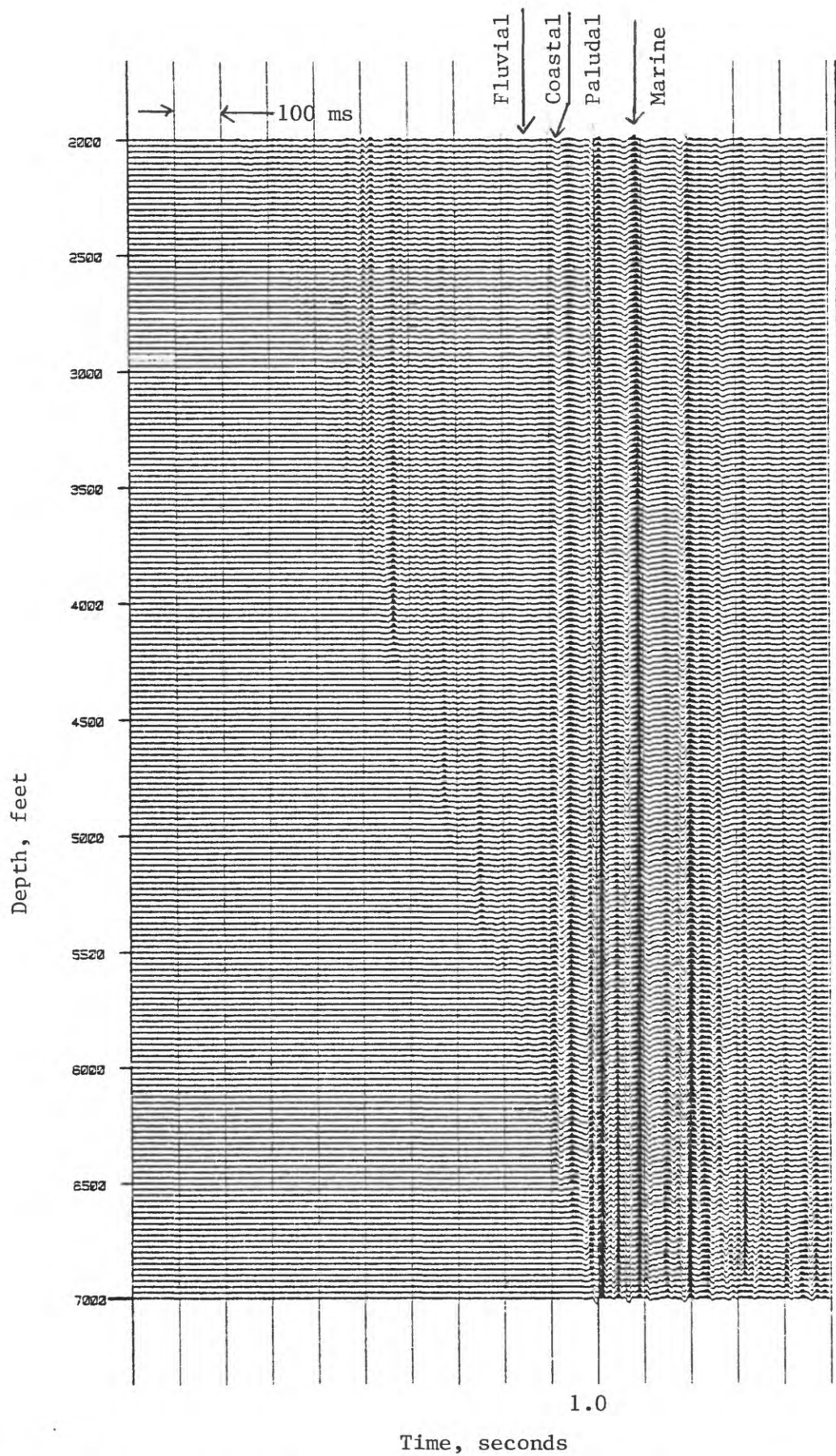


Figure 9.--Cumulative-summed vertical component of upgoing waves at MWX-3 from SL-1.

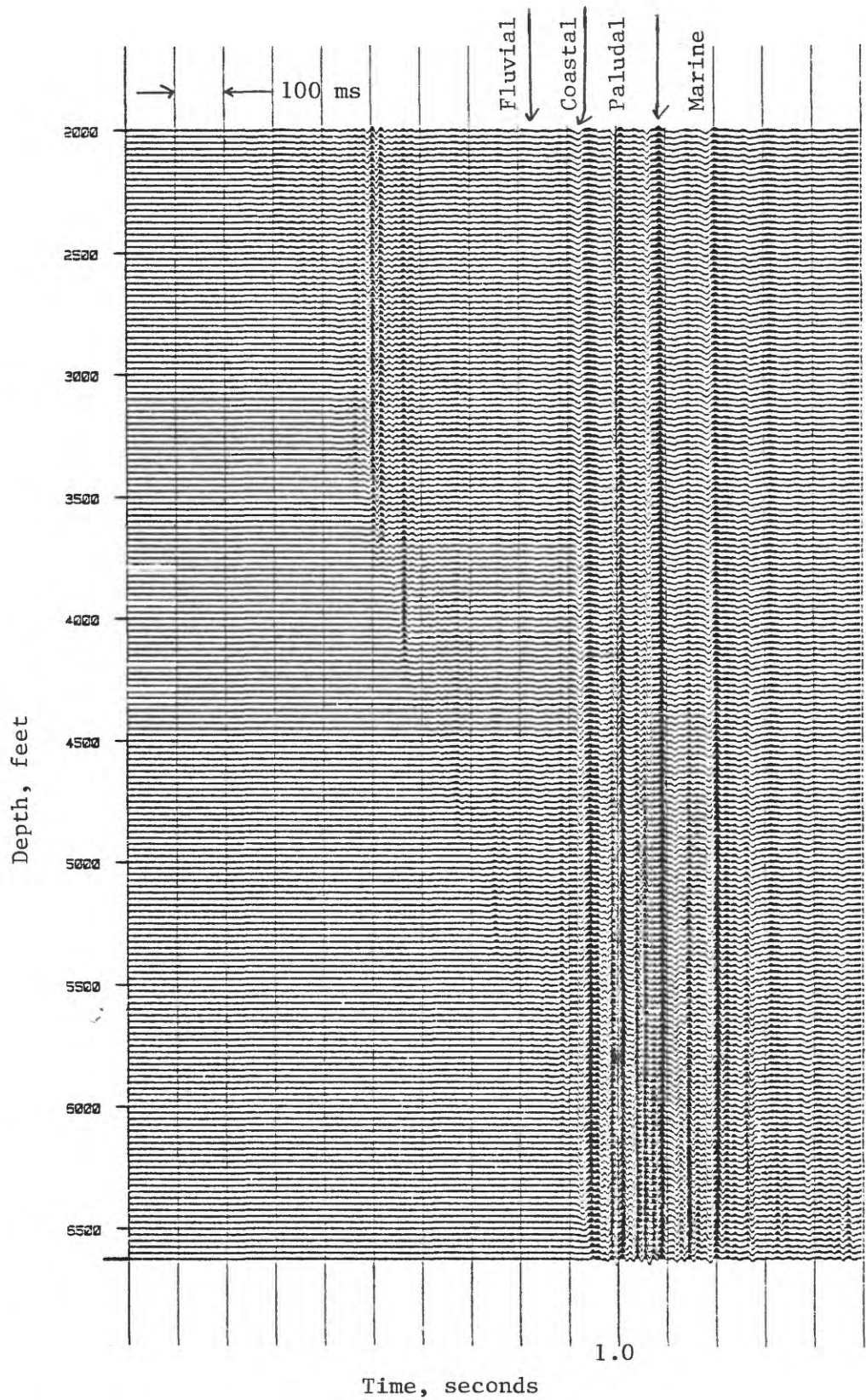


Figure 10.--Cumulative-summed vertical component of upgoing waves at MWX-2 from SL-1.



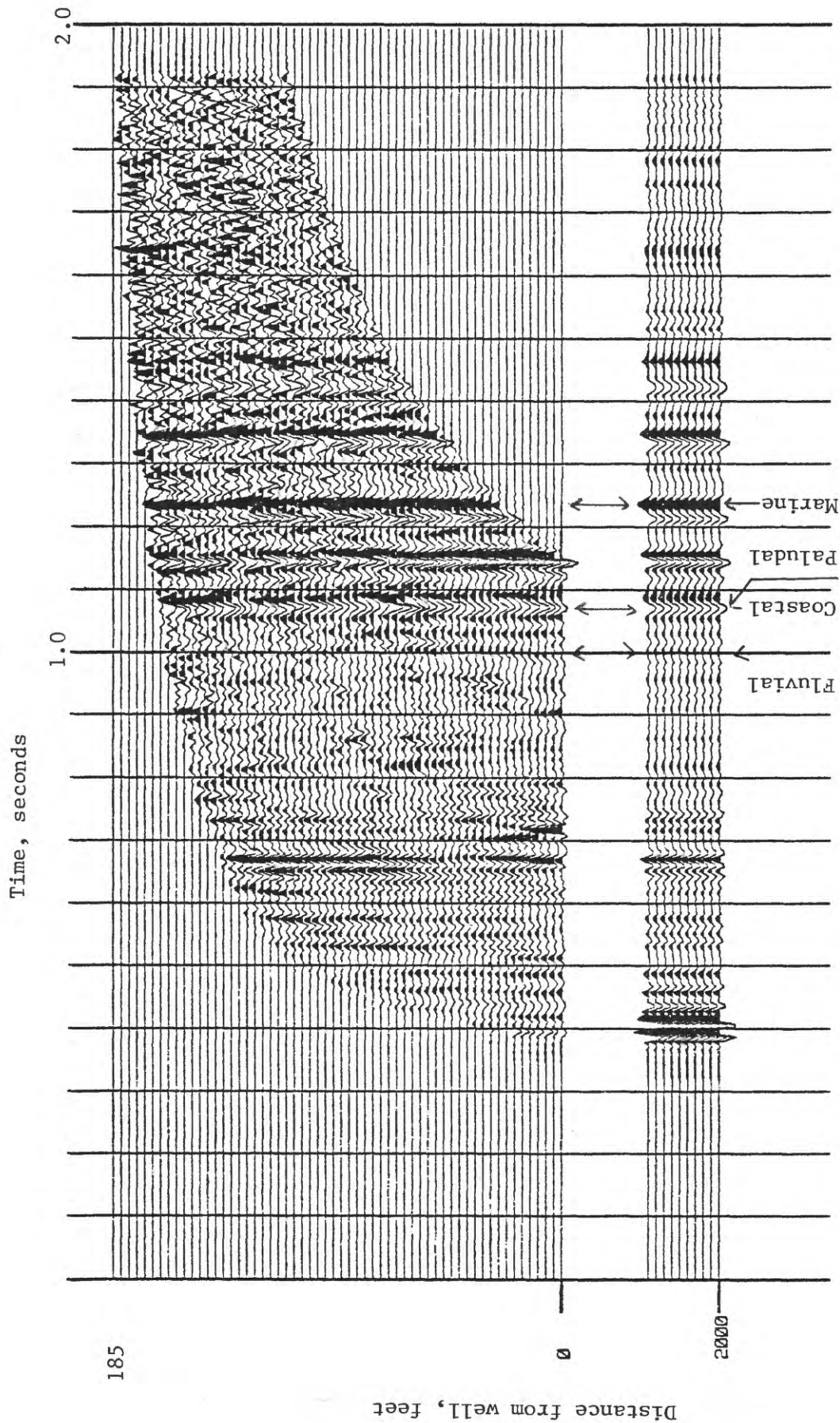


Figure 11.--Cumulative-summed and laterally stacked, vertical-component upgoing waves at MWX-3 from SL-1.  
Left: cumulative summation; right: lateral stacking.



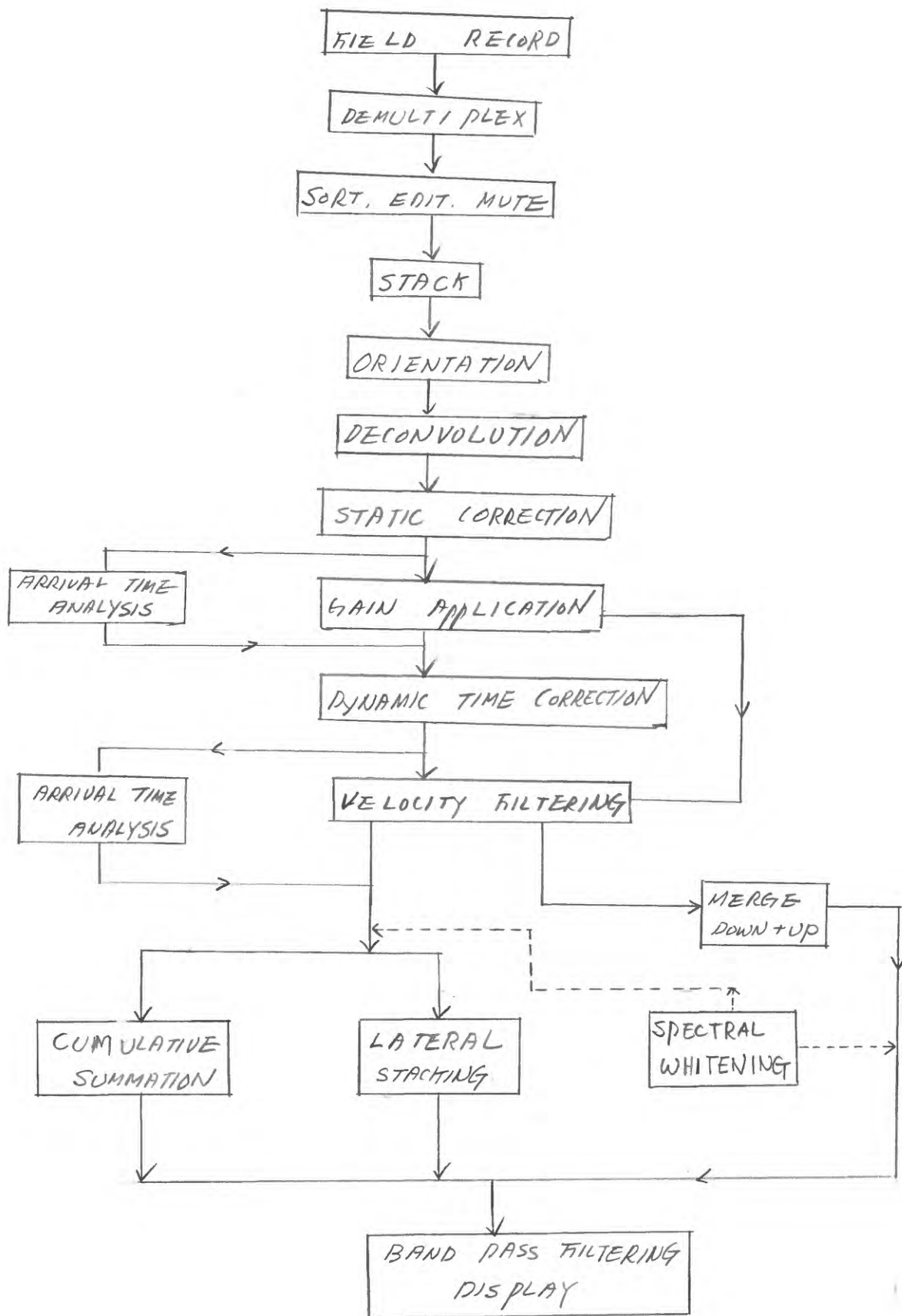


Figure 12.--Processing flow sheet for far-offset VSP data. Dotted line indicates the optional processing steps.

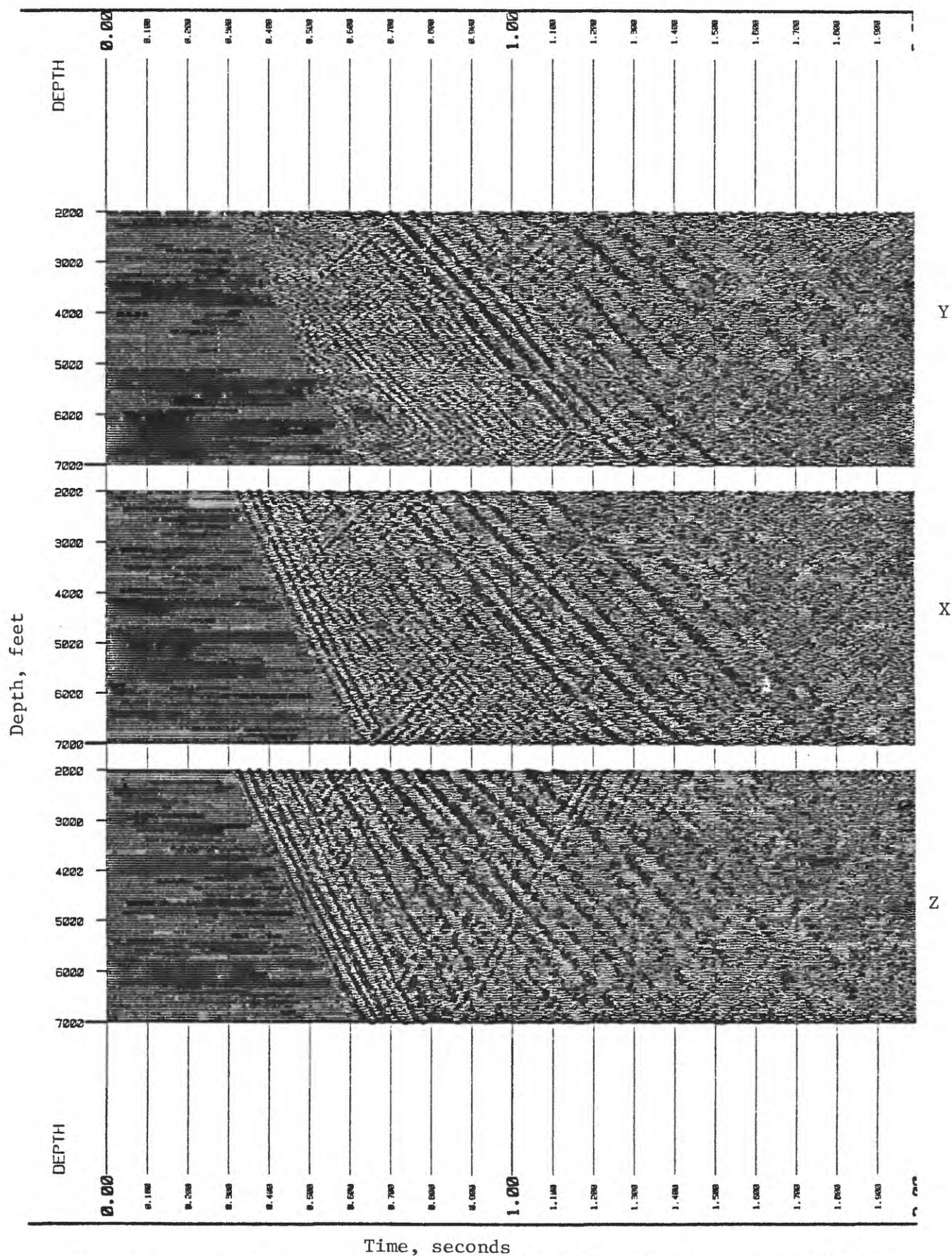


Figure 13.--Oriented, three-component data at MWX-3 from SL-2, reverse polarity.

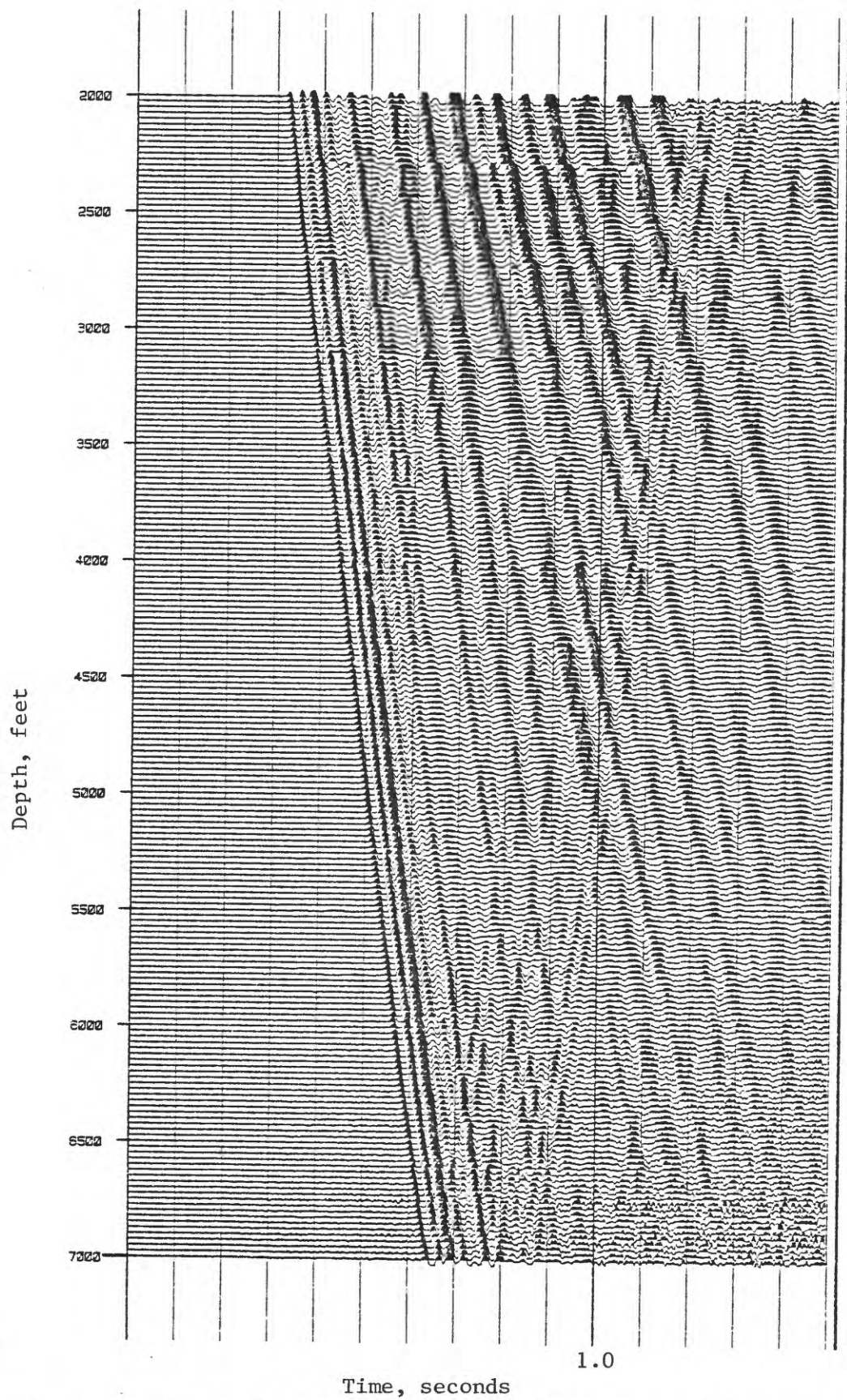


Figure 14.--Expanded version of the vertical-component data shown in fig. 13, reverse polarity.

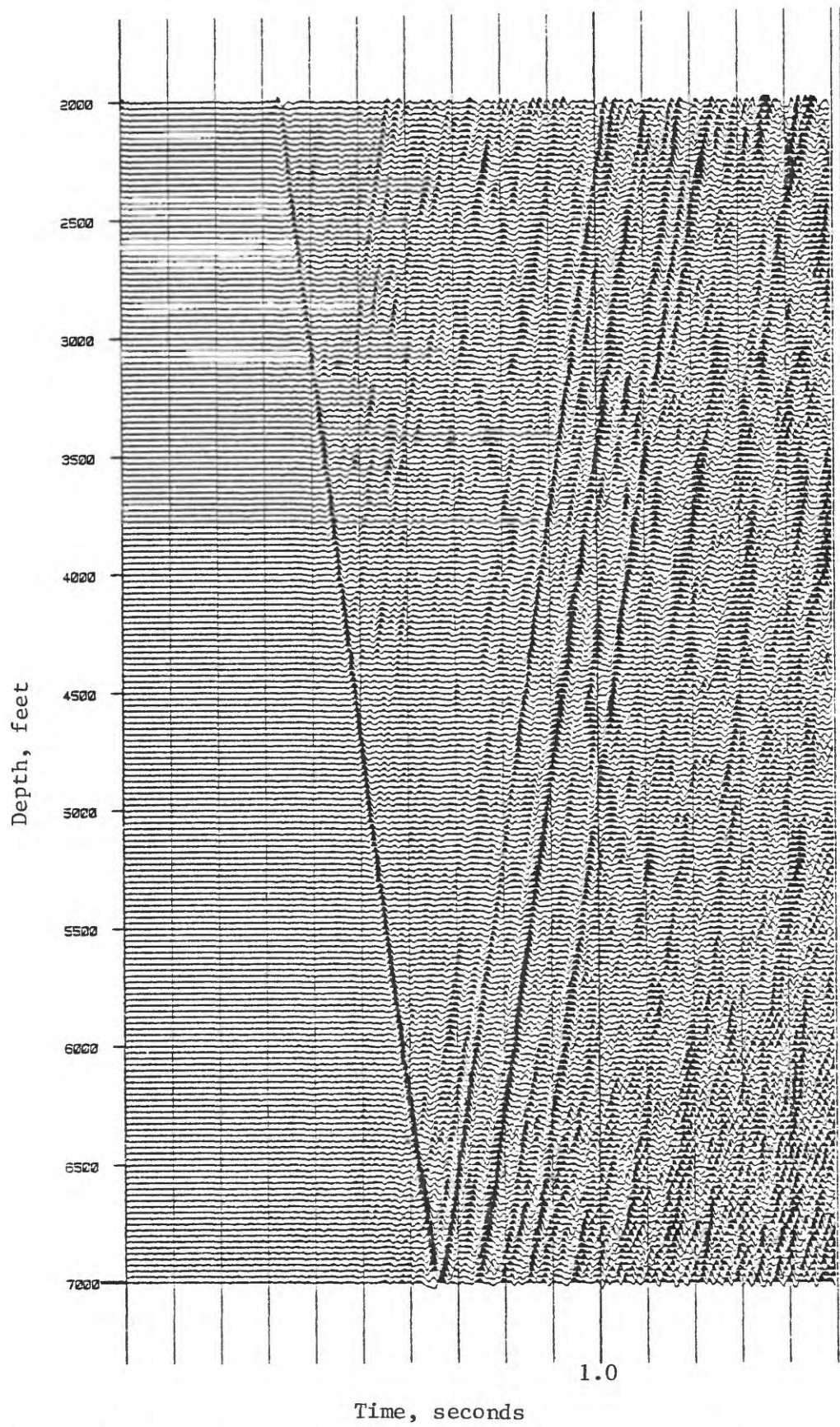


Figure 15.--Merged, vertical-component data at MWX-3 from SL-2.



Assuming the three-component data are available, the VSP data can be analyzed in any direction of interest by a coordinate transformation. One of the orientations of interest is the direction of the first-arrival P-wave particle motion and the perpendicular direction to the P-wave motion. Figure 16 shows the schematic diagram of the procedure. Then, by a coordinate transformation, we can show that

$$V_1 = V_z \sin \theta + V_x \cos \theta$$

$$V_2 = V_z \cos \theta - V_x \sin \theta,$$

where  $V_x$ ,  $V_z$  is the X- and Z-component of the data, respectively, and  $V_1$ ,  $V_2$  is the component along 1- and 2-direction, respectively. The angle can be approximately estimated by,

$$\theta = \tan^{-1} \left[ \frac{2 \int_{T_1}^{T_2} V_x V_z dt}{\int_{T_1}^{T_2} (V_x^2 - V_z^2) dt} \right]$$

where  $T_1$  and  $T_2$  are the time window for the first P-wave arrival. This is the same technique used to orient the data (Lee, 1984c).

Figure 17 shows merged  $V_1$  component data. The purpose for the highly reduced downgoing P-wave in this figure was to examine the converted upgoing SV-wave at the acoustic boundaries of interest. The strong converted SV-wave can be seen clearly near the unconformity (about 3,800 ft), and numerous other converted waves can be identified.

Figure 18 shows the laterally stacked and cumulatively summed, vertical-component data; figure 19 shows the SH-wave (Y-component data). The reflected P-wave near 1,140 ms looks truncated at about 500 ft away from the wellhead in figure 18. The same truncation near 2,300 ms can also be observed in figure 19. This amplitude variation with the lateral distance is the main ingredient for interpreting lenticular sand bodies in the lower coastal interval.

#### Source Location 3 (SL-3)

The general processing steps for SL-3 are identical to those for SL-2 shown in figure 12. The stacked vertical component is shown in figure 20. As mentioned in the data acquisition section, the data above 3,025 ft were not recorded due to a malfunction of the airgun at this source location. Furthermore, the low-frequency appearance of the data can be attributed to the muddy conditions at this source location. The merged section, shown in figure 21, indicates that there were some reliable reflections. However, the quality of the processed data is inferior to that shown in figure 15. Figure 22 shows the merged SH-waves; this component data is not very reliable due to the poor signal-to-noise ratio. By comparing figures 21 and 22, one could conclude that the timing changes (caused by movement of the source location) has a more pronounced effect on the shear wave.

The laterally stacked VSP data are shown in figure 23.

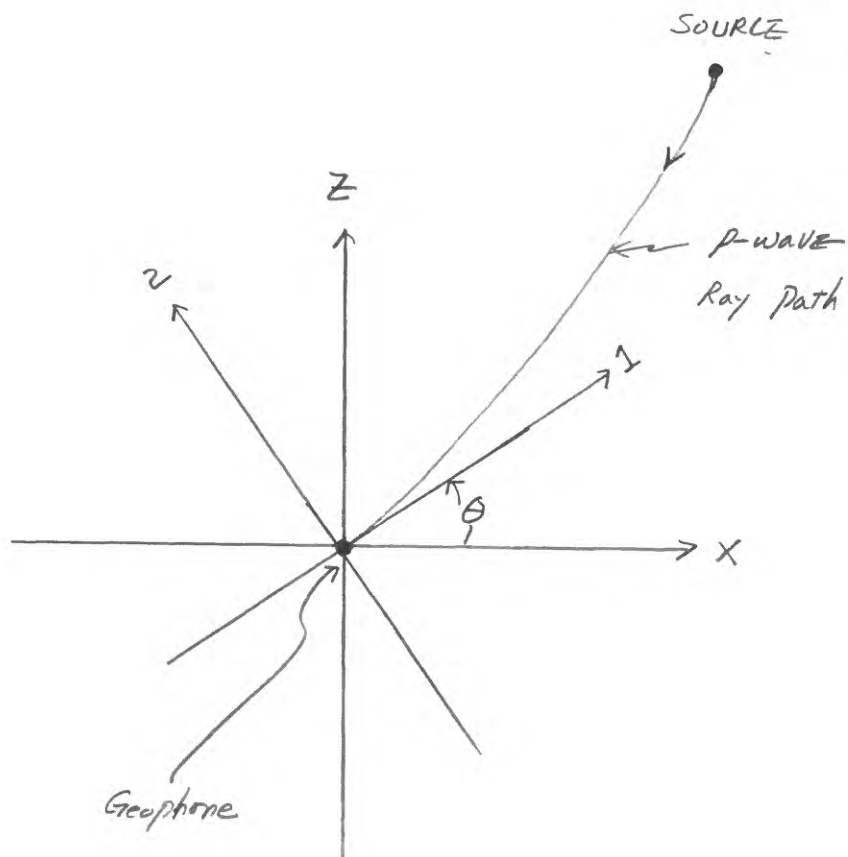


Figure 16.--Schematic diagram of P-wave ray path and coordinate transformation.

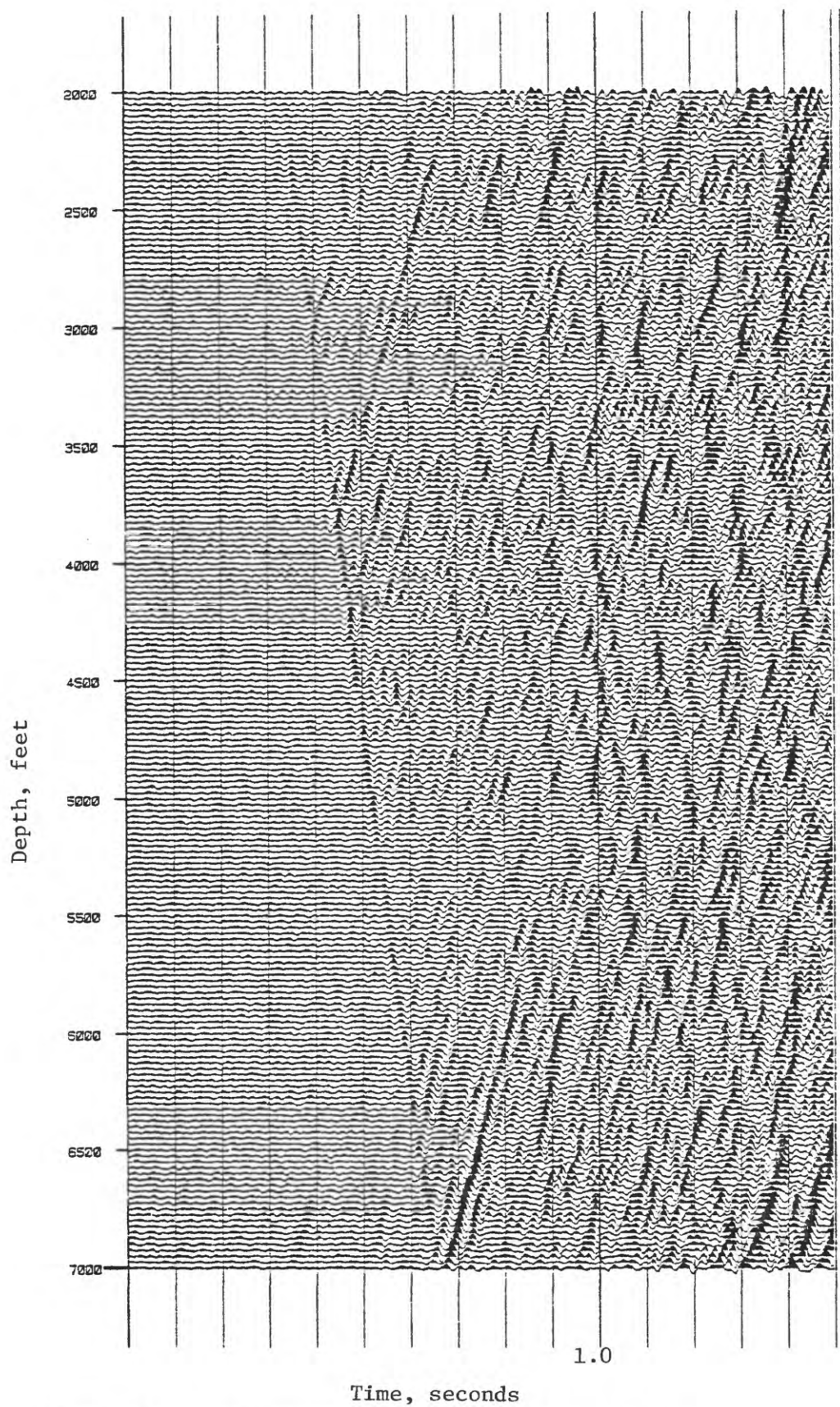


Figure 17.--V<sub>1</sub>-component data at MWX-3 from SL-2.

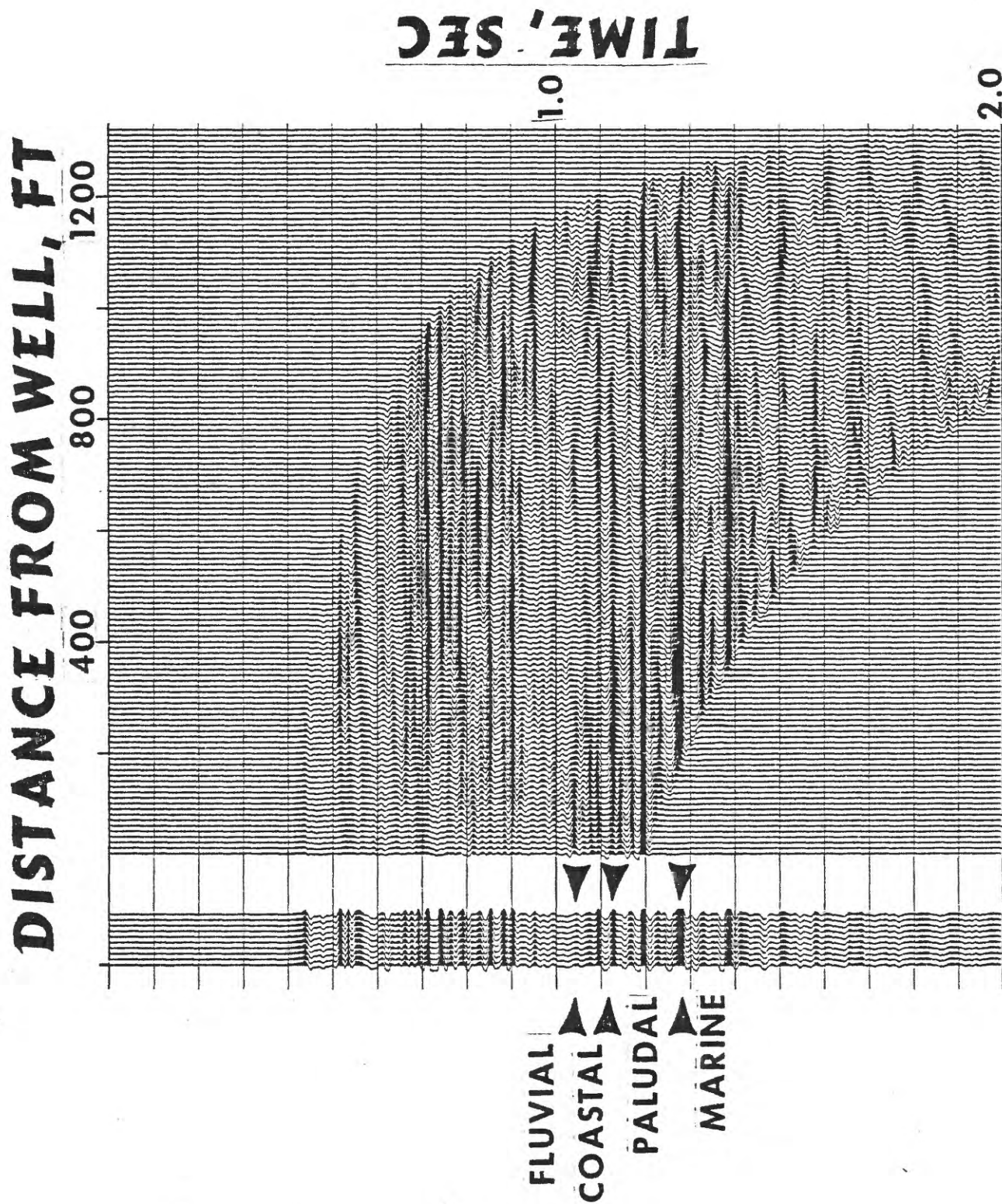


Figure 18.--Cumulative-summed and laterally stacked vertical-component upgoing waves at MWX-3 from SL-2. Left: cumulative summation; right: lateral stacking.



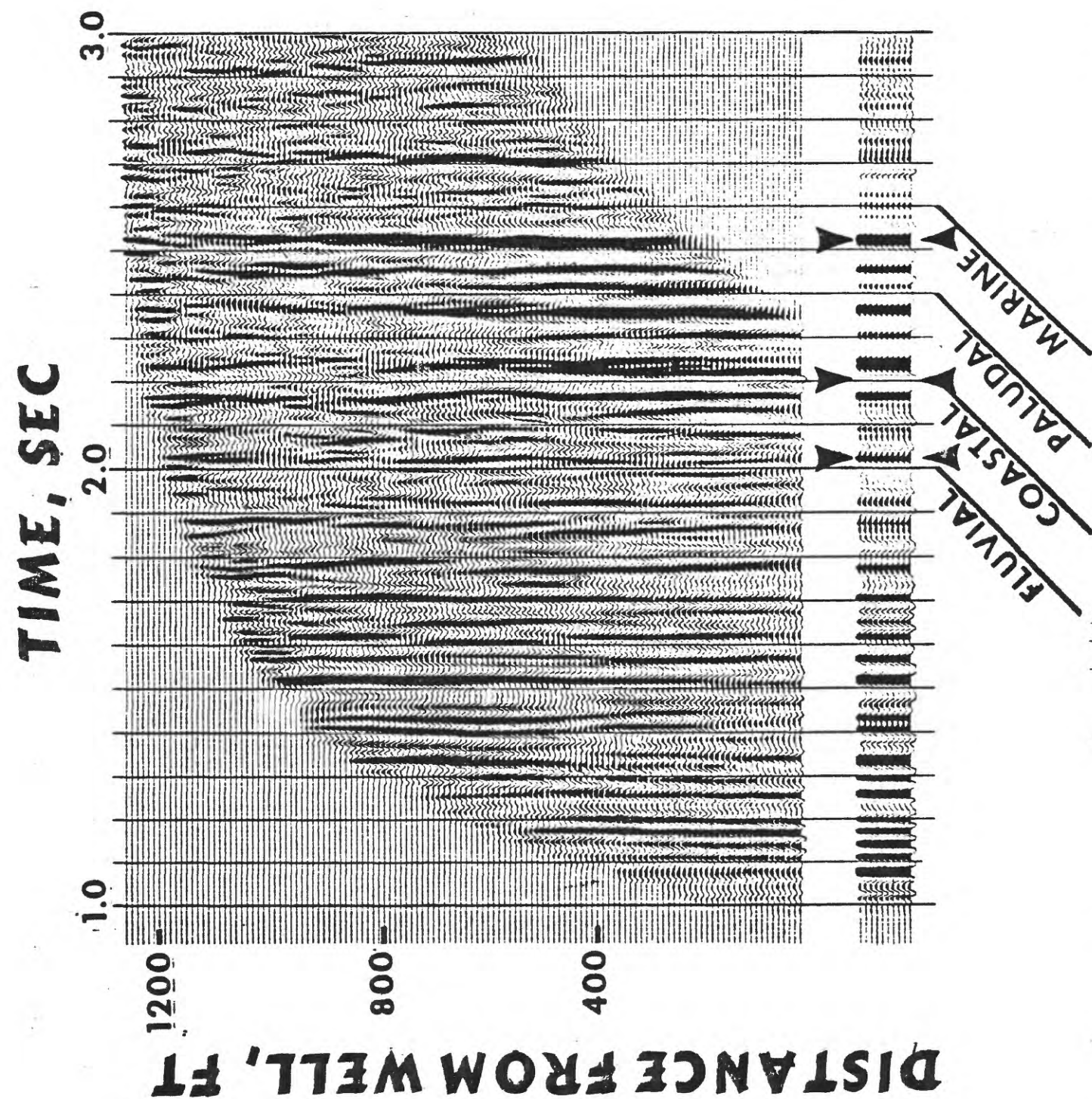


Figure 19.--Cumulative-summed and laterally stacked Y-component (SH-wave) data at MWX-3 from SL-2.  
Left: cumulative summation; right: lateral stacking.

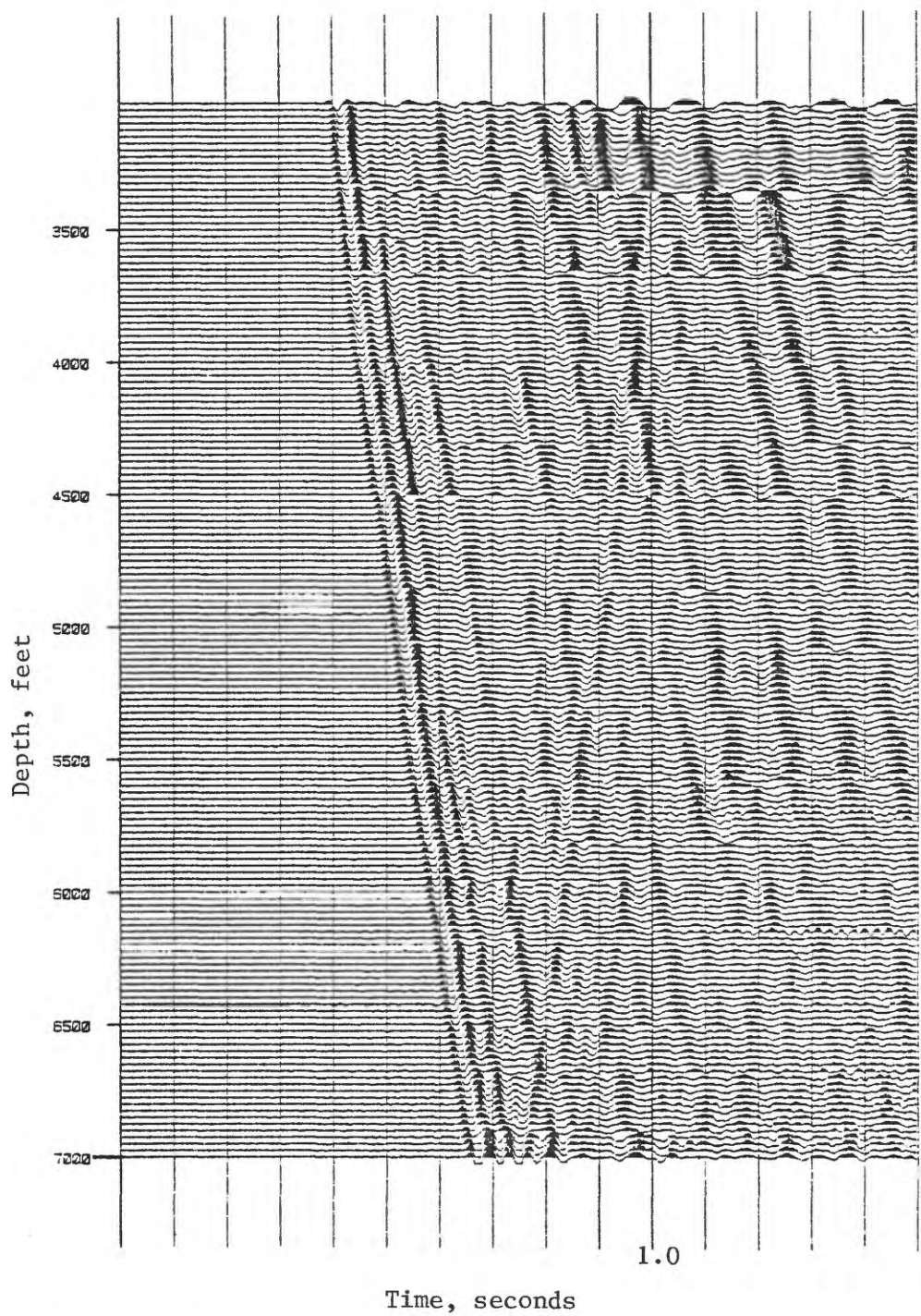


Figure 20.--Stacked, vertical-component data at MWX-3 from SL-3, reverse polarity.

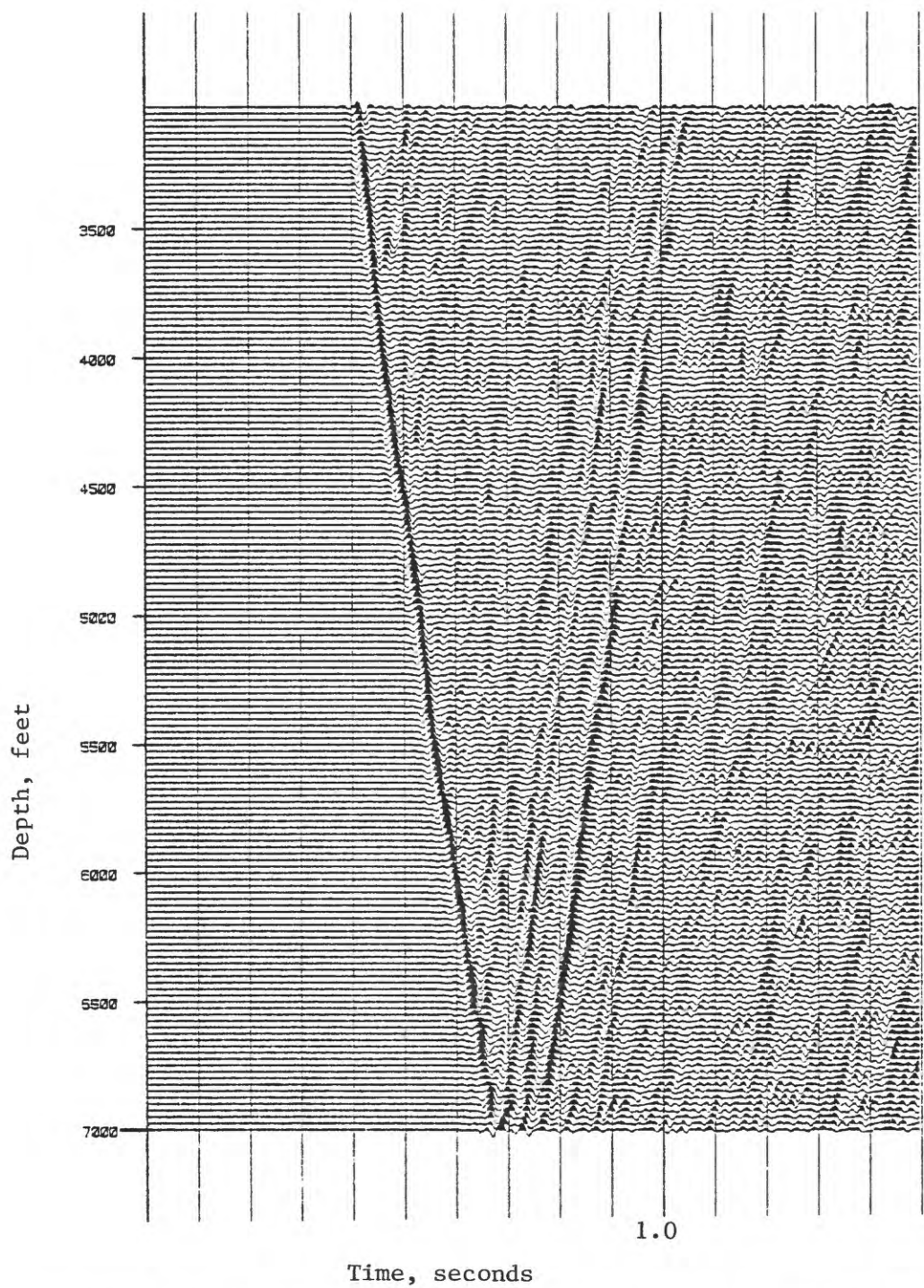


Figure 21.--Merged, vertical-component data at MWX-3 from SL-3.

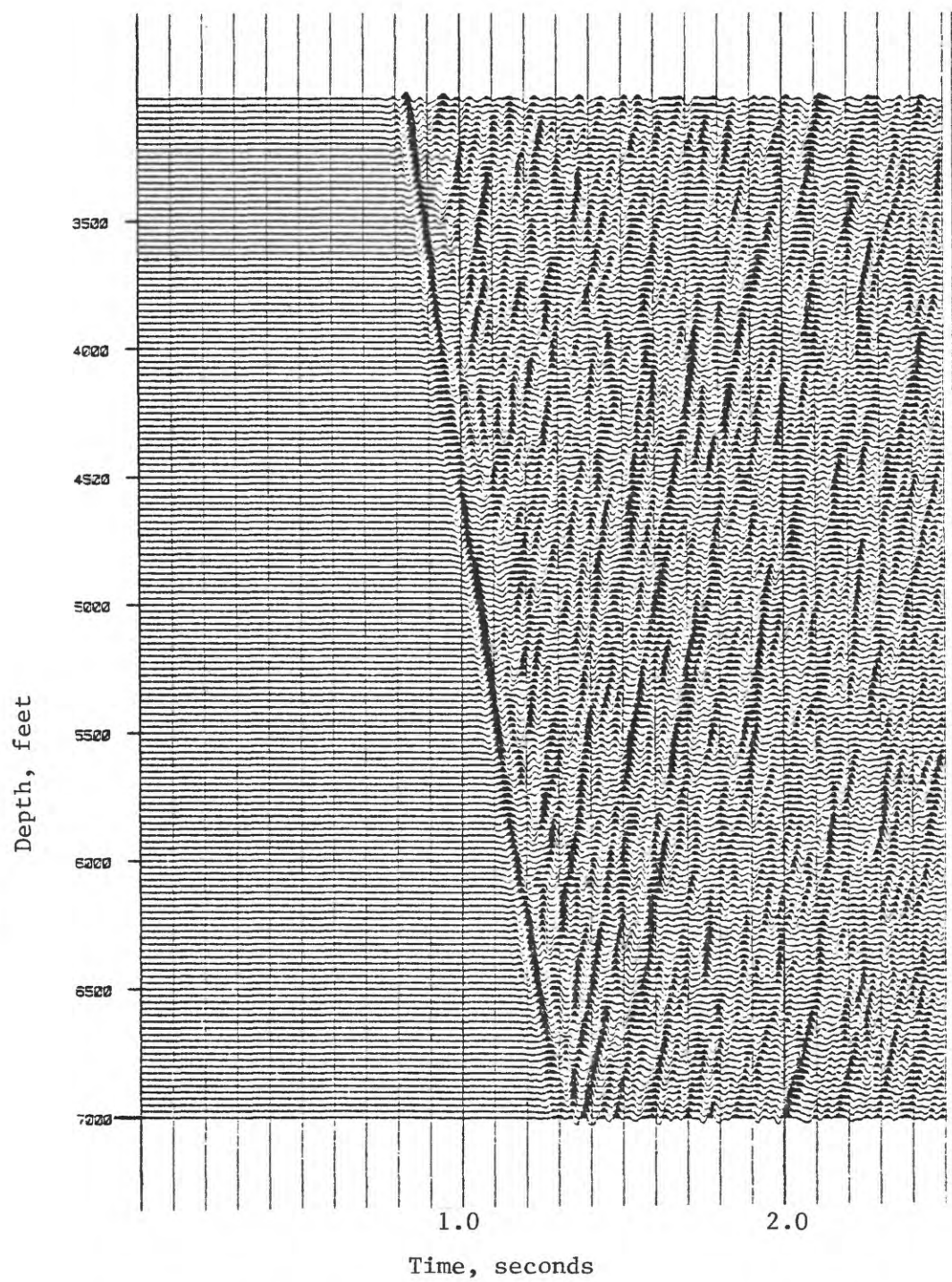


Figure 22.--Merged, Y-component data at MWX-3 from SL-3.



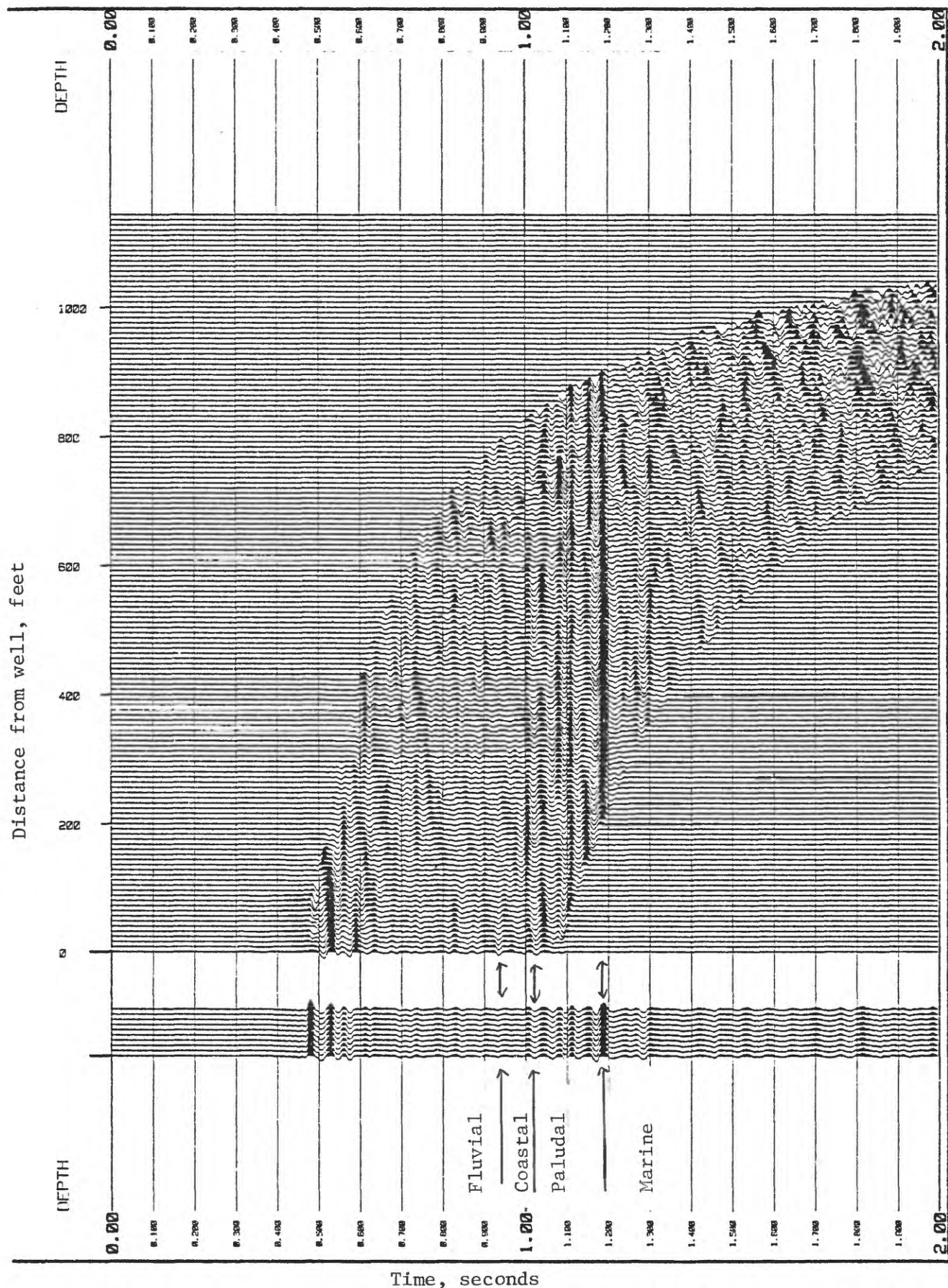


Figure 23.--Cumulative-summed and laterally stacked vertical-component upgoing waves at MWX-3 from SL-3. Left: cumulative summation; right: lateral stacking.

#### Source Location 4 (SL-4)

The general processing steps applied to this data set are shown in figure 12. The stacked, oriented, three-component data, shown in figure 24, are the worst of the data sets acquired during the azimuthal survey. Most of the problems were attributed to the soft ground condition at this source location. The differences in arrival times compared to that shown in figure 13 are remarkable, considering that the two sources were located on opposite sides of the MWX-3 well at almost the same distance.

The merged VSP section is shown in figure 25. This figure indicates that the processing was adequate, but the data set was inferior and would cause problems in delineating the lenticular-type sand bodies at a later time. Different processing sequences and techniques to enhance the signal-to-noise ratio were attempted but to no avail.

The laterally stacked VSP data are shown in figure 26. In this version, we tried to keep the frequency bandwidth as broad as that from SL-2. To increase the interpretability of the data, a frequency-domain spectral whitening technique (Lee, 1985b) was applied prior to the lateral stacking. This result is shown in figure 27. This process was also applied in figure 25 before plotting.

#### CONCLUSIONS

The quality of the VSP data acquired during this survey was degraded by adverse field conditions at the source locations. Combined with the limitation of well availability for the azimuthal survey, the quality control during the field work was not sufficient to produce high-quality VSP data for interpretation of the coastal sand bodies. Careful processing, however, provided a usable data set for further investigation of the possibility of detecting and delineating lenticular-type sand bodies by VSP techniques.

The processing steps adopted in this study are most promising and would be applicable to similar VSP data. Variable norm deconvolution proved to be the best technique for improving signal-to-noise ratio and converting the complicated reverberatory downgoing wave into a simple wavelet for these data.

Unfortunately, although data processing techniques can enhance seismic signals in the data, they cannot create signals which have been lost during the data acquisition. Therefore, the most critical factor to be considered in any future experiments is adequate field procedure for data acquisition and careful selection of source locations.

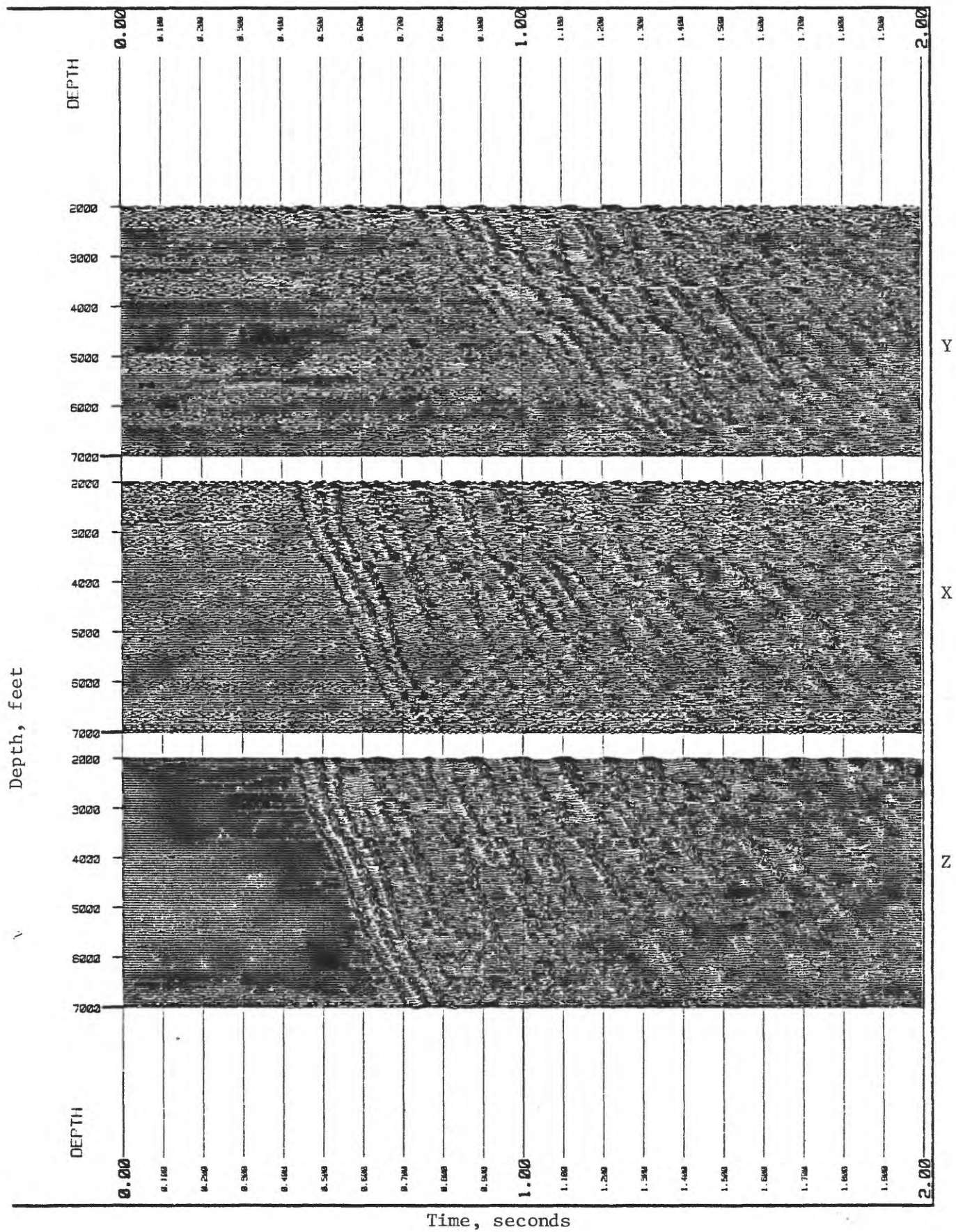


Figure 24.--Oriented, three-component data at MWX-3 from SL-4, reverse polarity.



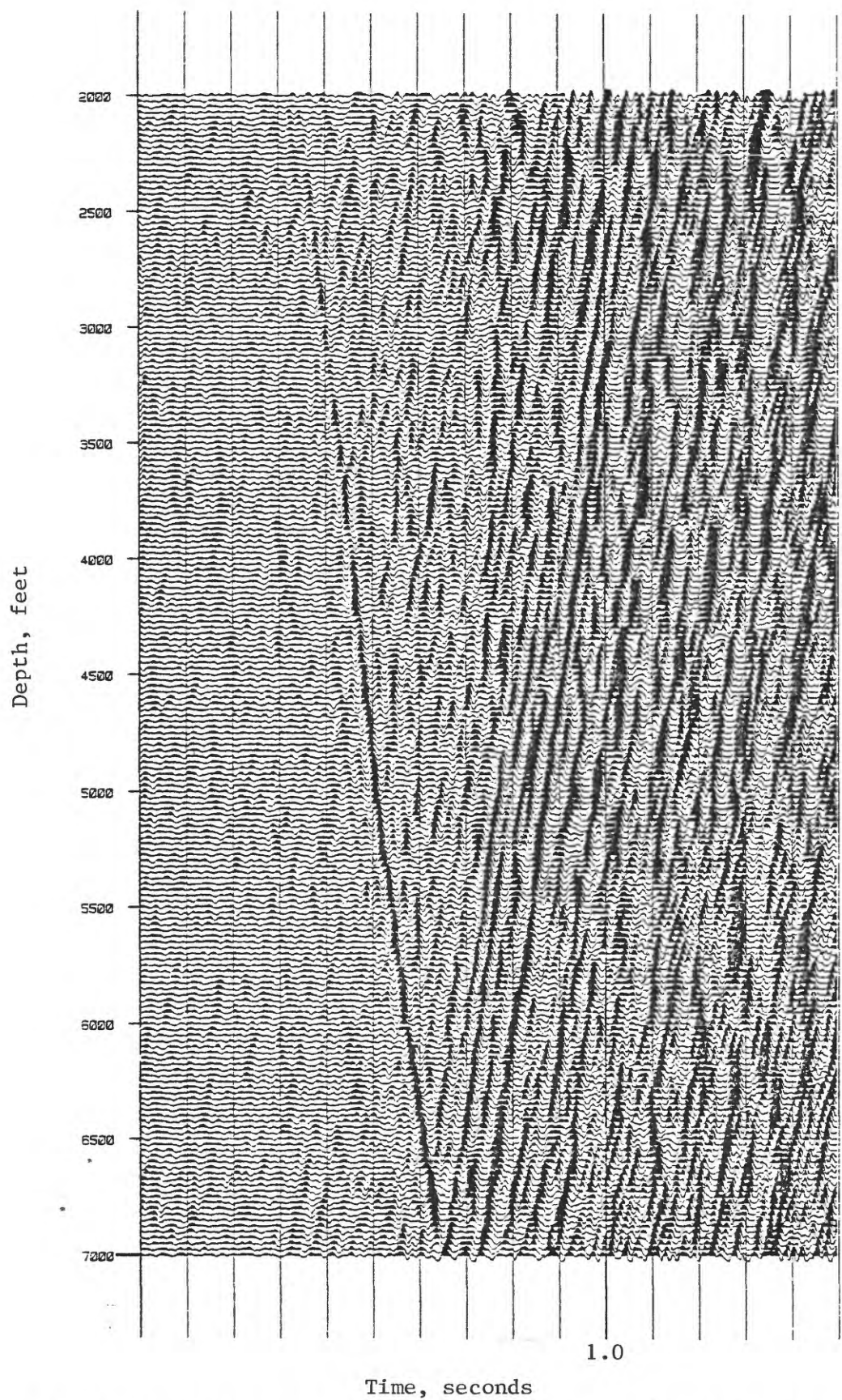


Figure 25.--Merged, vertical-component data at MWX-3 from SL-4, reverse polarity.



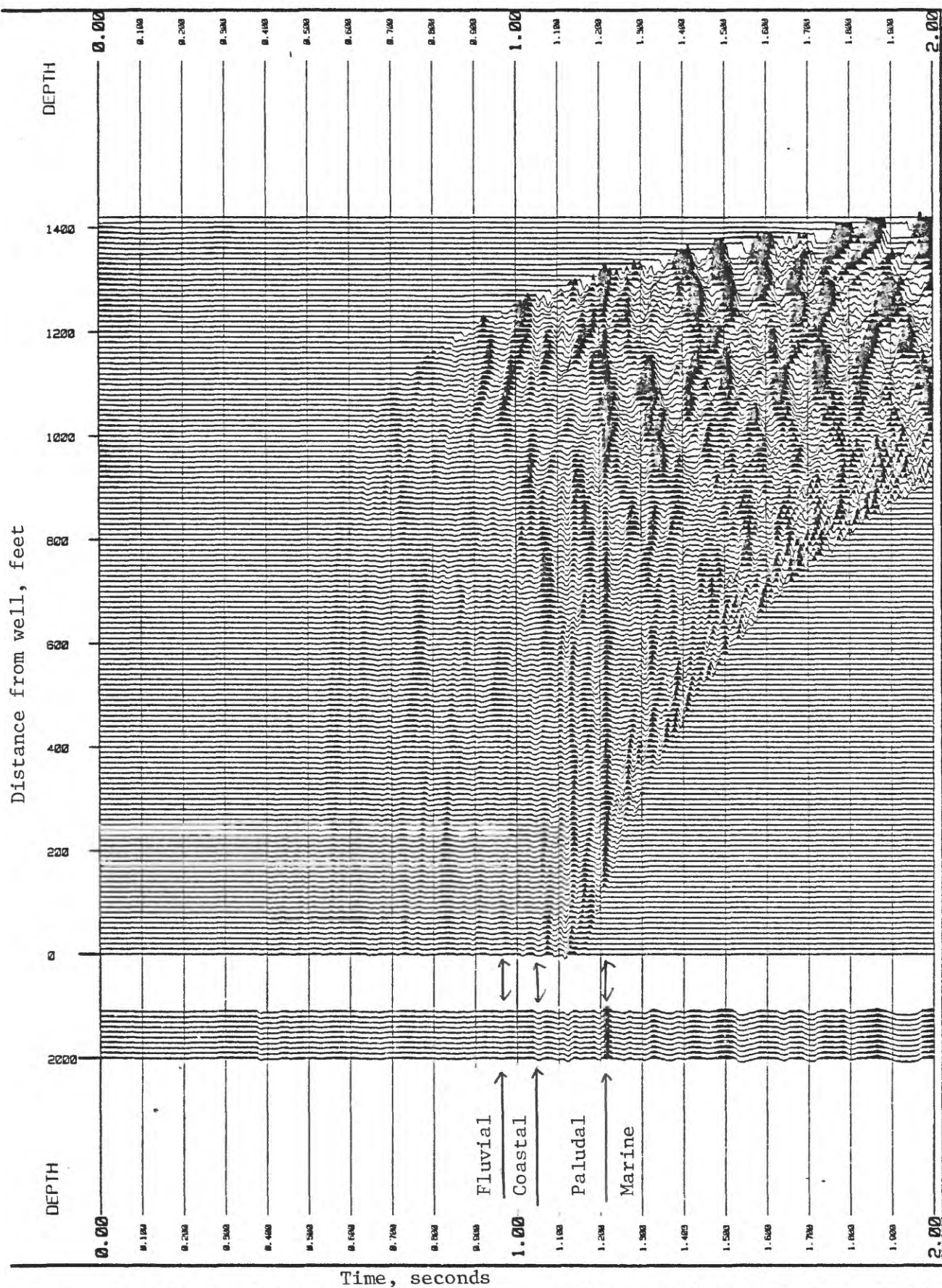


Figure 26.--Cumulative-summed and laterally stacked, vertical-component upgoing waves at MWX-3 from SL-4. Left: cumulative summation; right: lateral stacking.

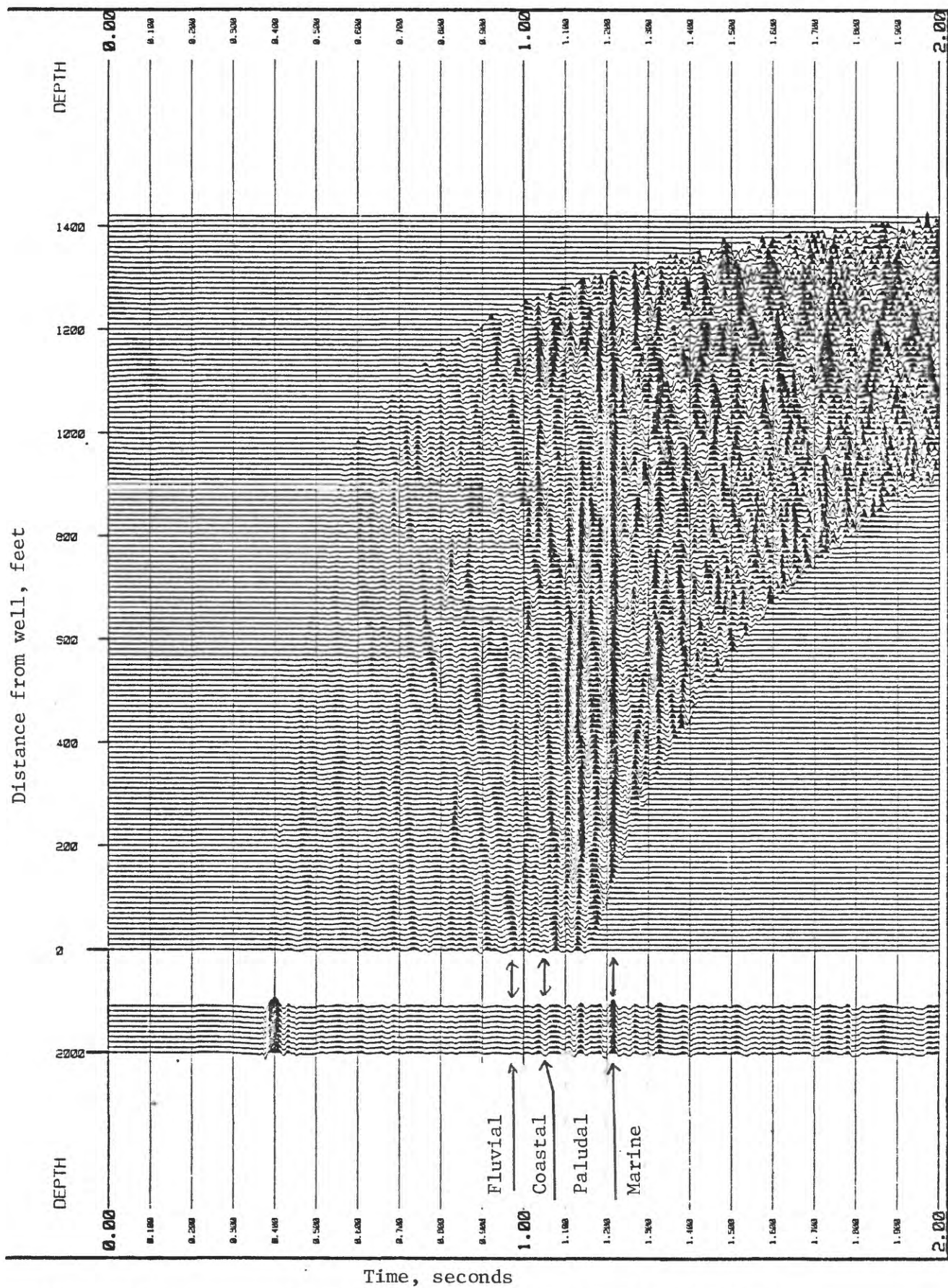


Figure 27.--Same as fig. 26 with application of spectral whitening.

#### REFERENCES CITED

- Gray, W. C., 1979, Variable norm deconvolution: Stanford University Ph.D. Thesis.
- Lee, M. W., 1984a, Vertical seismic profiles at the multi-well experiment site, Garfield County, Colorado: U.S. Geological Survey Open-File Report 84-168, 57 p.
- Lee, M. W., 1984b, Delineation of lenticular-type sand bodies by the vertical seismic profiling method: U.S. Geological Survey Open-File Report 84-265, 92 p.
- Lee, M. W., 1984c, Processing of vertical seismic profile data, in Simaan, M., ed., Advances in geophysical data processing: Greenwich, JAI Press, Inc., p. 129-160.
- Lee, M. W., 1985a, Interpretation of azimuthal vertical seismic profile data at multi-well experiment site, Garfield County, Colorado: U.S. Geological Survey Open-File Report, in press.
- Lee, M. W., 1985b, Spectral whitening in the frequency domain: U.S. Geological Survey Open-File Report, in preparation.
- Lee, M. W., and Balch, A. H., 1983, Computer processing of vertical seismic profile data: Geophysics, v. 48, no. 3, p. 272-287.
- Searls, C. A., Lee, M. W., Miller, J. J., Albright, J. N., Fried, Jonathan, and Applegate, J. K., 1983, A coordinated seismic study of the multi-well experiment site: Society of Petroleum Engineers of AIME, SPE/DOE 1983, Symposium on Low Permeability Gas Reservoirs, Paper no. 11613, 10 p.
- Wiggins, R. A., 1978, Minimum entropy deconvolution: Geoprospection, v. 16, p. 21-35.